

NAL PROPOSAL No. 0027

Correspondent: J. Rosen
Department of Physics
University of Rochester
Rochester, New York

FTS/Off-net: 716-546-4900
275-2121

PROPOSAL TO STUDY THE SMALL ANGLE NEUTRAL BEAM
USING A V SPECTROMETER

J. Rosen, T. Ferbel, B. Gobbi, S. Shapiro, P. Slattery, B. Werner
University of Rochester

June, 1970

PROPOSAL TO STUDY THE SMALL ANGLE NEUTRAL BEAM
USING A V SPECTROMETER

Drs. J. Rosen (Correspondent), T. Ferbel, B. Gobbi, S. Shapiro, P. Slattery,
 B. Werner

University of Rochester

Abstract

We propose to construct a V Spectrometer to survey the N.A.L. small angle neutral beam. The system will employ conservative techniques and will be a suitably scaled and modified version of the kind of V spectrometer which has been successfully employed for K_L^0 measurements at lower energy machines (e.g. $K_L^0 \rightarrow \pi^\pm e^\mp \nu$, K_S^0 regeneration and CP violation experiments). We discuss a new scheme wherein the large beam energies made available by N.A.L. will facilitate neutron, anti neutron and K_L^0 measurements with the same basic apparatus. We propose to

- a. Measure the absolute flux of n , \bar{n} and K_L^0 in the range (40 - 200) BeV/c with good momentum resolution ($\sim 1\%$).
- b. Make precision total cross section measurements with the above particles using hydrogen and various complex nuclei for transmission targets.
- c. Measure the presently unknown radiative process
 $K^{*0} \rightarrow K^+ + \gamma$.
- d. Extend and improve upon a variety of kaon physics experiments.

I. Introduction

We propose to construct a neutral beam V spectrometer. This would contain a large aperture magnet and associated counters, spark chambers, computer and ancillary equipment. The general class of event that will be studied is

$$X^0 \rightarrow A^+ + B^-.$$

The known physical processes which provide reactions of this sort in a neutral beam devoid of short lived particles are classified below.

1. a. K_L^0 decays in flight
- b. K_S^0 decays downstream of a regenerator placed in the K_L^0 beam.
2. V 's produced in a neutral beam target. Reactions of particular interest are:

- a. Reactions in the Coulomb field of a heavy nucleus.

$$(i) \quad n + \gamma \rightarrow \Delta^0(1236) \rightarrow \pi^- + p$$

$$(ii) \quad \bar{n} + \gamma \rightarrow \bar{\Delta}^0(1236) \rightarrow \pi^+ + \bar{p}$$

$$(iii) \quad K_L^0 + \gamma \rightarrow \frac{1}{\sqrt{2}} \left(\begin{array}{c} K_S^{*0} \\ \downarrow \\ K^+ + \pi^- \end{array} + \begin{array}{c} \bar{K}_S^{*0} \\ \downarrow \\ K^- + \pi^+ \end{array} \right) \quad (\text{approximately}).$$

These Coulomb reactions are expected to be reasonably copious at N.A.L. energies. This should not be too surprising.

The key

point is that at N.A.L. energies the minimum momentum transfer required for the above reactions is adequately small.

$$q_{\min} = \frac{m_A^2 - m_N^2}{2 p_{\text{inc}}} \quad \left(\text{or} \quad \frac{m_{K^*}^2 - m_K^2}{2 p_{\text{inc}}} \right).$$

The physics of the Coulomb process is described in an appended report.

Y. Nagashima and J. Rosen, UC-875-105.

- 2 -

Reaction (ii) is simply the anti particle version of (i). Reaction (i) is essentially the transpose of a reaction long studied in photon beams. To good accuracy then, the rates of reactions (i) and (ii) can be regarded as known. We do not propose to get new physics by measuring these processes as such. We propose to use these processes as a detection mechanism for flux and total cross section measurement. Certain coherent nuclear processes may interfere weakly with these Coulomb processes and we can learn something about their physics by varying nuclear targets and studying dynamical details such as mass spectra and decay distributions.

Reaction (iii) has not yet been studied but is of great theoretical interest. Presumably, the simplest hadrons are the pseudoscalar mesons (M) and the vector mesons (V). The radiative transitions $V \rightarrow M + \gamma$ are of fundamental importance and it is worth comparing the various transitions. To date only the $\omega^0 \rightarrow \pi^0 + \gamma$ process has been measured ($\pm 10\%$). During the next year we will carry out an A.B.S. experiment (# 531, 400 hours), to measure the rate of $\phi^- \rightarrow \pi^- + \gamma$. This will use the same Coulomb field technique envisaged in this proposal. This proposal is both technically and physically relevant to our N.A.L. proposal and will be discussed further in the body of the proposal. We hope to extract a measurement of $K^{*0} \rightarrow K^0 + \gamma$ to better than 5% accuracy from the N.A.L. work.

We continue with our summary of V induced reactions.

b. Coherent reactions with nuclei. By coherent we mean those reactions which leave the nucleus in its ground state. The most significant example is



Reactions of this type are of interest in their own right and will be recorded in this experiment. We expect such reactions to be ~ 10 times

smaller than the Coulomb reactions (i) and (ii), at least for heavy nuclei such as Pb. The differences in mass, decay and production angle distributions permit relatively easy separation. The principal reason for the dominance of the Coulomb reaction can be traced to the fact that coherent nuclear reactions are strongly damped by nuclear attenuation. The effective nuclear number for Pb, A_{eff} is ≈ 20 (rather than 206). These processes scale like $(A_{\text{eff}})^2$. The Coulomb process scales like Z^2 and there is very little damping because only a small portion of the Coulomb interaction takes place with impact parameters less than the nuclear radius.

These remarks are not casual speculations. We have carefully surveyed the situation at energies ≈ 25 BeV. Some data for pions and protons incident on hydrogen and several nuclei are available. The Coulomb field reaction mechanism (Primakoff Effect) has already been experimentally studied in connection with π^0 and η^0 production by photon beams. Relevant theoretical and experimental work has been carried out concerning coherent vector meson production and K_S^0 regeneration. This work demonstrates the essential soundness of our ideas concerning nuclear coherence, diffractive and Coulomb dissociation and the adequacy of the optical model for parametrization.

Extrapolation to N.A.L. energies gives cause for optimism. This optimism is engendered by two considerations. We do not expect hadron total cross sections to change markedly at N.A.L. energies. Stated differently, hadron mean free paths in nuclear matter are expected to be about the same. Hence the damping and A_{eff} predicted by optical model calculation should be reliable. Furthermore, we expect that the mean multiplicity of particles produced by hadron reactions will continue to increase. There is support for this from Cosmic Ray data. Therefore the fraction of low multiplicity reactions which might complicate triggering

or analysis, should be smaller.

c. Incoherent nuclear reactions. The bulk of hadron reactions in complex nuclei are incoherent, i.e. the nucleus is highly excited with appreciable nucleon and γ ray emission. Most of these reactions produce large high energy particle multiplicity as well. Since we intend to emphasize heavy targets such as Pb for the main experimentation, this particle multiplicity will be exacerbated by secondary reactions initiated in the large nucleus. Thus, most incoherent reactions result in an explosive fragmentation which can be rejected in triggering.

The Coulomb process 2a - (i) is calculated to be ~ 15 mb/(Pb nucleus). More details can be found in the appended report. The process results in a well directed small angle, energetic V. The total interaction cross section of Pb is ≈ 1500 mb. We estimate that ≈ 10 mb of these reactions will result in sufficiently low multiplicity and excitation so as to provide a source of trigger background.

Before turning to a description of the apparatus and a more detailed discussion of the program of studies, a few general remarks may be in order.

We have already alluded to a rich and comprehensive program of neutron and kaon physics that can be carried out within the framework of the V spectrometer. We would like to emphasize the versatility of the arrangement.

The first order of priorities should be the job of measuring beam composition, flux and total cross sections. This, after all, is the kind of information which can facilitate the design of more subtle second generation experiments. Nevertheless, physics fallout may be expected. We aspire to become involved in some, but not all of the subsequent physics program, some of which is already apparent.

A strong feature of the V spectrometer is its compatibility with multiple use of the beam. Exclusive of thick transmission targets and regenerators, only a few grams of interaction material will be placed in the beam. Space, rigging and other resources permitting, other experimentation could take place downstream with little or no discomfort.

II. Experimental Equipment

The principal elements are schematically indicated in Figure 1. These are

1. Neutral Beam
2. Target, Target counter system
3. Vertex Hodoscope
4. Gas Cerenkov Counter (Hydrogen)
5. Wide Aperture Magnet
6. Trigger Hodoscopes
7. Wire Spark Chambers
- not indicated { 8. Dedicated Computer and Magnetic Tape System
9. Miscellaneous Equipment - Trailer, gas and pulsing systems, Electronic logic, etc.

1. Neutral Beam

A well collimated, small angle neutral beam is required. A flux of 10^7 neutrons in the range (40 - 200) BeV/c and a beam cross section of about 1 (inch)² is suitable. We envisage a 1000 foot beam with an intermediate station (having tunnel access with beam off). This station would contain remotely controlled horizontal and vertical collimating jaws of hevimet or perhaps brass, a sweeping magnet and provisions for inserting transmission samples or filters.

2. Target, Target Counter System

We will not discuss the set up modifications necessary to perform decay in flight or regeneration experiments. These are straightforward

extensions of procedures already used at existing machines. Instead we will concentrate on the procedures for studying coherent nuclear or Coulomb reactions.

We propose to use $1/4$ radiation length targets - mostly Pb, occasionally Cu, Al or C. These will be sandwiched between a $1/16$ " thick veto and a $1/32$ " thick trigger counter. Since the K_S^0 mean free path is 2m at 40 BeV/c, we will not confuse target produced V's with kaon decays.

The target will be surrounded on all sides, except for entrance and exit holes on the beam axis, with a veto complex which will serve to suppress uninteresting nuclear reactions either on the basis of large particle multiplicity or by nuclear fragmentation. This procedure could be compromised by excessive beam halo or room background. A schematic layout of the veto complex (model I) which we will use in our A.G.S. experiment, is shown in Figure 2. This arrangement has been constructed and will be tested at A.G.S. this summer. Many questions concerning trigger background suppression will be quantitatively answered at that time. The N.A.L. neutral beam version will be suitably modified.

3. Vertex Hodoscope

Following the target complex we will place a scintillation hodoscope (both horizontal and vertical planes) to establish the initial coordinates of the V. This will be constructed from 1.5 mm cylindrical scintillating rods staggered in such a way as to overlap by 0.5 mm. In effect this will provide bin intervals of 0.5 mm width. A bank of 40 elements will cover a width of 4.0 cm.

4. Gas Cerenkov Counter

The bulk of the upstream region will be filled with a 15 m. 1 atmosphere threshold Cerenkov counter. The basic gas fill will be hydrogen. A $\beta = 1$ particle will provide 200 photons under these conditions. The Cerenkov angle will be 1° . The threshold energies will be 57, 30, 8.4 BeV for protons, kaons, and pions respectively.

The counter will have thin windows and aluminized mylar reflectors for light collection. The counter walls will be strong enough so that with the installation of temporary end windows, the counter can be rough pumped for filling purposes. A Fabry-Perot interferometer device will be attached to monitor the index of refraction. A slight overpressure will be maintained in the manner employed with spark chambers. The counter will be sectorized into quadrants by a "petal" arrangement of the primary reflectors.

5. Wide Aperture Magnet

For the purposes of the present design we describe a magnet which is suitable, recognizing that if funds and power were available it might be wise to purchase a somewhat larger one.

$$48 \text{ D } 48$$

$$\text{gap} = 24''$$

$$\int B dl = 20 \text{ Kg m}$$

$$\text{transverse momentum kick} = 0.6 \text{ BeV/c}.$$

6. Trigger Hodoscopes

We do not have a detailed design at this time. No exotic triggering is foreseen.

We will require 2 and only 2 charged particles passing through the system. We expect these hodoscopes to play a large role in the pattern recognition program for the wire spark chambers. Previous experience has

shown that this pattern recognition problem is one of the more tedious aspects of wire chamber operation.

7. Wire Spark Chambers

We will not present the details of their construction or operation at this time.

We would like to point out that we have extensive experience with this technique. We have just completed an experiment which recorded 6 million triggers and employed 12 wire planes. The chambers were completely fabricated in Rochester. We are equipped to wind chambers of arbitrary size. Data was recorded with the aid of the Rochester owned Honeywell DDP-516 computer and ancillary magnetostrictive equipment.

It is conceivable that the experiment could be improved from the point of view of speed of data recording by a modification of item (7). This would involve the use of very large area Charpak chambers instead of wire chambers. This would be very expensive and the successful utilization of such large systems is not yet demonstrated. We will not go into details concerning the pro's and con's at this time. Suffice it to say that we retain open minds and view with interest new developments, particularly the recent work of Fisher and Shibata at B.N.L. on a new type of chamber which combines some of the best features of both approaches.

8. Dedicated Computer

We are in the process of purchasing a PDP - 15 system.

We would probably request a link to a large time sharing central computer for selective on-line analysis. This could be supplemented or replaced by rapid turn-around off line computing on an N.A.L. large computer.

Division of Responsibilities

We would expect N.A.L. to provide:

Neutral Beam

Magnet

Venting and safety equipment for Cerenkov counter

Power, rigging and other "traditional" services.

We would be delighted to secure some in-house collaboration. If this experiment were to achieve the status of facility it would be highly desirable to have local staff who would be familiar with its components and who could aid other potential users.

We are quite amenable to collaborating with other users. Another institution could take partial or complete responsibility for items 3, 4, and 6 for example.

III. Experimental Program

A. Neutron and Anti-Neutron Flux Measurements

We begin using a 1.5 g Pb target. In the range (10-200) BeV/c the Coulomb process $n + \gamma \rightarrow \Delta^0 \rightarrow \pi^- + p$ has a useful cross section of roughly 5 mb/Pb nucleus. See appended report, Table I. This gives an event rate

$$(10^7 \text{ neut/pulse}) \frac{(1.5 \text{ cm}^2)(.6 \times 10^{24})}{206} (5 \times 10^{-27} \text{ cm}^2) = 250/\text{pulse}.$$

Detection efficiency which is largely a question of the solid angle acceptance of magnet will be $\approx 50\%$. Therefore the useful yield will be $\sim 100/\text{pulse}$.

This is more than adequate for flux measurements and should suffice for total cross section measurements. A few weeks ($\sim 10^5$ pulses) -- 10^7 events distributed over various transmission target in-out operations.

should give 1% cross sections over, say 5 BeV/c intervals.

Our spark chambers will have a recovery time of a few m sec.

1. Background

Although the useful yield of high energy $\pi^- + p$ pairs from the Coulomb process is ~ 5 mb, it must be noted that the Pb interaction cross section is approximately geometric i.e. ≈ 1500 mb. Now the great bulk of this results in very large multiplicity and nuclear fragmentation. In our background estimates we conservatively estimate that only the outer rim of ~ 500 mb projected area can be regarded as hydrogen-like i.e. free of secondary interactions, reabsorption and remultiplication. At A.G.S. energies it is observed that pp collisions result in single energetic $p\pi^-$ pairs for less than 1% of the interactions. Thus we expect trigger background from the nuclear rim with an effective cross section of a few mb or less. Direct experimental data will be available shortly.

The coherent process $n + A \rightarrow A + N^*(1470)$ should contribute a few mb of cross section but this is interesting rather than debilitating.

2. Resolution

The final kinematical analysis will involve the wire chamber measurement of π^- and p momentum. The coherent events will be signaturred by a sharp peak on a plot of events versus transverse momentum transfer. The sharp peak will be largely contained inside $q(\text{transverse}) \approx 30$ MeV/c. Incoherent background will have an average $q(\text{transverse}) \sim 300$ MeV/c.

Angle resolution $\sim 1 \text{ mm}/20 \text{ m} = 5 \times 10^{-5}$.

Momentum resolution will be $\sim 1\%$. For example, a 100 BeV/c proton will bend by $(0.6 \text{ BeV/c}/100 \text{ BeV/c}) = 6 \text{ mr}$. This gives $\delta p/p = \delta\theta/\theta \approx 1\%$.

The uncertainty in $p(\text{transverse})$ resulting from angle uncertainty will be $p \delta\theta \approx 5 \text{ MeV/c}$.

The actual limit on transverse momentum resolution comes from multiple Coulomb scattering, principally in the $1/4$ radiation length target. There are 2 particles produced on the average $1/2$ way into the target. Therefore the uncertainty produced by the target on p_{\perp} is ~ 10 MeV/c. Thus we see that the transverse resolution is adequate for resolving the sharp coherent spike.

3. Further Comments

On the average the proton will have $3x$ the momentum of the pion. The Δ^0 is produced with a degree of alignment which results in a $1 + 3 \sin^2 \theta$ decay distribution where θ is the proton direction in the Δ^0 C.M. This is another useful characteristic signature of the process.

The Coulomb Δ^0 excitation process is quite large and it will be unnecessary to use Cerenkov information. We can simply assume that the energetic particle is a proton if positive and is an anti-proton if negative. For incident neutrons below ~ 15 BeV/c, the Cerenkov counter will check this point.

Let us discuss this further. Decays in flight (kaons) are signaturred by the fact that the V does not originate in the target. It is easy to establish what fraction of the time (negligibly small) that they accidentally originate in the target. We are then confronted with only three possibilities $K^{\pm} \pi^{\mp}$, $p \pi^{-}$ and $\bar{p} \pi^{+}$ pairs. This is a consequence of baryon and strangeness conservation. Since the beam is dominantly neutrons, $p \pi^{-}$ pairs will predominate. The $K^{\pm} \pi^{\mp}$ pairs can be separated from the others in the kaon momentum range (40-60) BeV/c with the aid of the Cerenkov counter. If our expectation that the $K^{\pm} \pi^{\mp}$ pairs are dominantly produced by the Coulomb mechanism is verified, then the yield of $K^{\pm} \pi^{\mp}$ pairs at other energies can be predicted. That is, it can be predicted if we know the kaon flux. This is inferred from the decay in flight studies which are discussed below.

B. Decay in Flight Studies

With some relatively obvious modifications the system can be used to study decays in flight. The copious decays $K_L^0 \rightarrow \pi^\pm \ell^\mp \nu$ and the rare $K_L^0 \rightarrow \pi^+ \pi^-$ CP violating decays can be recorded and kinematically separated. The latter gives the flux in a straightforward fashion if the commonly accepted value for the parameter η^{+-} is used.

However, we should like to make the following argument. Measurements below ~ 10 BeV/c show that η^{+-} is energy independent to a few percent accuracy.

Perhaps there are other, energy dependent mechanisms for CP violation. Perhaps $\eta^{+-} = \eta^{+-}(0) + \alpha \gamma^2$. We will be in a position to test the constancy of η^{+-} under conditions where γ^2 is ~ 100 times larger than previously accessible. The point seems worth checking.

C. Regeneration Studies

By placing material in the beam and observing downstream decays the process of coherent K_S^0 regeneration can be measured at the highest accessible energies. This can provide the most stringent test of the Pomeranchuk theorem. Recall that this theorem states that for a given target (A), the total cross sections for the $\chi + A$ interaction approaches asymptotically the cross section for $\bar{\chi} + A$.

Now, given $K_L^0 (= \frac{1}{\sqrt{2}} [(1 + \epsilon)K^0 - (1 - \epsilon)\bar{K}^0])$ the regeneration amplitude is proportional to $(f - \bar{f})$, the difference between the complex forward scattering amplitudes for K^0 scattering and \bar{K}^0 scattering. The optical theorem states that the total cross section is proportional to the imaginary part of the forward scattering amplitude. Therefore in the Pomeranchuk limit, the regeneration factor $(f - \bar{f})$ should become purely real.

" 13 "

Now, the regeneration amplitude interferes with the $K_L^0 \rightarrow \pi^+ \pi^-$ amplitude so that both the magnitude and the phase of the regeneration amplitude can be measured. A very sensitive measurement can be made. The above argument is well known to those familiar with kaon physics.

Assuming that a reasonable regeneration amplitude can be found at high energies, the regeneration process can be used as a K_L^0 detection mechanism. Transmission measurements can be made after the fashion of the neutron work.

D. Further Experimentation

There are undoubtedly many exciting possibilities for experimentation that cannot be perceived at present. Some of these will be stimulated by the early results. However a few other experiments are already apparent. We briefly note these.

The Rubbia group at C.E.R.N. has recently reported an upper limit to K_S^0 electron regeneration. This effect is γ dependent and a factor 10 improvement can presumably be made at N.A.L.

Present upper limits on $K_L^0 \rightarrow \mu^+ \mu^-$ and $K_S^0 \rightarrow \mu^+ \mu^-$ are flirting with the edge of current theoretical predictions. Higher energy kaons can improve this situation markedly. Pion decays in flight can be choked off more easily.

IV. Concluding Remarks

Our principal present experimental effort is the A.G.S. experiment on $\pi^- + \gamma \rightarrow \rho^-$ alluded to earlier. We also plan to measure $p + \gamma \rightarrow \Delta^+ \rightarrow p + \pi^0$. The latter will directly relate to the proposed scheme of neutron detection. Testing will get underway this summer. This entire experiment was conceived as a natural precursor to the N.A.L. effort herein proposed.

This proposal is a brief one and we fully expect to submit additional

technical data. These will include references and background estimates contained in our A.G.S. proposal. Monte Carlo programs for efficiency, resolution momentum transfer, mass and decay distributions exist but we have not had time to modify them for this proposal.

We trust however, that this proposal serves to signal our interest, the nature of the physics and the technical scale of the program.

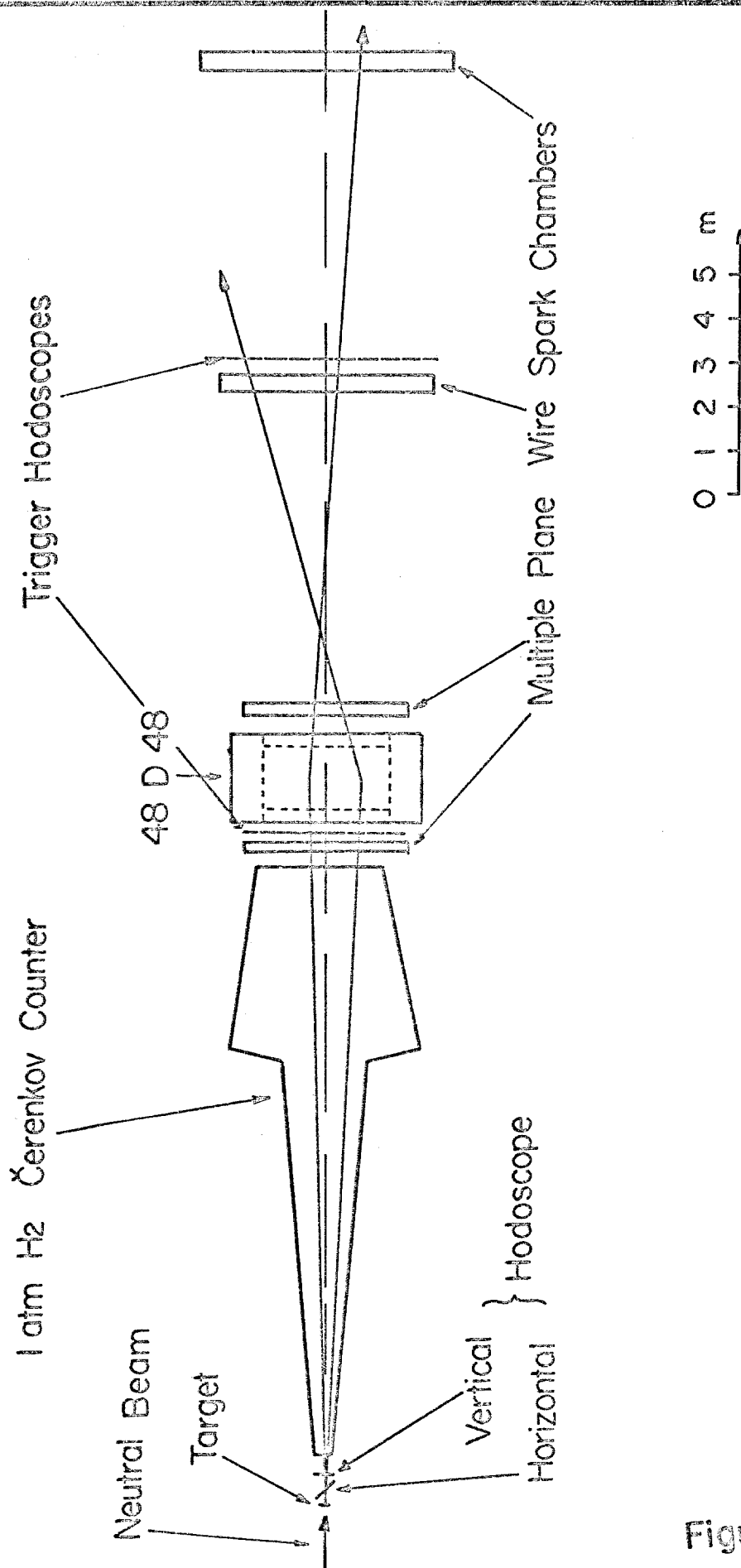


Figure 1

Veto Counters (Light Pipes Deleted) 7 PM's Req'd

-  Pb
-  Scintillator



FRONT VIEW
LOOKING DOWNSTREAM

TOP VIEW

SECTION A-A

Target

A

A

Report Number ---- UR-875-295

Coulomb Production of $N^*(1236)$ #

Y. Nagashima[†] and J. L. Rosen

Department of Physics, University of Rochester, Rochester, N. Y.

November 3, 1969

Contract Number AT(30-1)-875

Abstract

The cross section for $N + \gamma_C \rightarrow N^*$ in the Coulomb field of a nucleus is calculated. This process may provide the basis for a new scheme for high energy neutron detection with excellent energy and directional properties. The cross section is directly related to the well established process of N^* photoproduction $\gamma + N \rightarrow N^*$ so that the absolute efficiency of the neutron detection scheme may be predicted with some reliability. The possibility of constructing a tagged neutron or antineutron beam is also briefly discussed.

Work supported by the United States Atomic Energy Commission

[†] Present address: Lauritsen Lab., Cal Tech, Pasadena, Calif.

Individual copies will be supplied as long as the supply lasts.

A. Introduction

A discussion of the process of Coulomb production of N^* closely parallels that of the Primakoff effect $\gamma + \gamma_C \rightarrow \pi^0 (\eta^0)$.¹ Most of the remarks concerning the conditions for coherence, nuclear form factor and the effects of nuclear self absorption and coherent background carry over to the present case with minor modification. The specific process of N^* production has already been considered by Good and Walker² in a qualitative way. We shall discuss the effect in more detail and comment on the possible exploitation of the process in connection with very high energy neutron experiments.

A similar process, $\pi^\pm + \gamma \rightarrow \rho^\pm$ has been considered by Pomeranchuk and Shmushkevich³ and Ferman and Drell.⁴ The analogous formulae worked out by these authors will be noted for comparison. The same formulae apply to the processes $K^\pm + \gamma_C \rightarrow K^{*\pm}(890)$ and $K^0 + \gamma_C \rightarrow K^{*0}(890)$.⁴

In the $N + \gamma_C \rightarrow N^*(1236)$ process the rates for an incident neutron or proton are equal as a consequence of the pure isovector nature of the transition. The formulae presented are applicable to the experimentally contentious case of $\Sigma + \gamma_C \rightarrow \Sigma^*$ ($J^\pi = 3/2^+$) as well.

B. Cross Section and Decay Angular Distribution

Figure 1 is a Feynman graph of the process which also serves to define the dynamical variables. We assume that the transition matrix element is pure magnetic dipole. The algebraic manipulations are deferred to the Appendix.⁵

$$H = \frac{\lambda(q^2)}{m} \bar{u}_\nu(F) \epsilon_{\mu\nu\rho\sigma} \frac{p_\rho}{M} q_\sigma u(p_1) \left(\frac{Mm}{E\varepsilon} \right)^{\frac{1}{2}} A_\mu \quad (1)$$

where A_μ is provided by the nuclear Coulomb field (in the laboratory system).

$$A_\mu = (\vec{A}, A_0) = [0, iZeF(q^2)/q^+{}^2] \quad (2)$$

The nuclear form factor has the property that $F(0) = 1$. The quantity $\lambda(q^2)$ is the effective coupling constant. Conventional $\gamma + N \rightarrow N + \pi$ and $e + N \rightarrow e + N + \pi$ experiments in the region of the $N^*(1236)$ mass show that the magnetic dipole approximation is a good one and that the further approximation $\lambda(q^2) = \lambda(0) \cdot F_M(q^2)$ where $F_M(q^2)$ is the proton magnetic form factor is also valid.

At some future time it may be provident to include small corrections to Eq. (1) to account for the q^2 dependence of λ and the contributions of E2 and longitudinal photon processes. The factor $\epsilon_{\mu\nu\rho\sigma}$ is the 4-dimensional permutation symbol and $u_\nu(P)$ is the Rarita-Schwinger spinor describing the spin 3/2 field.

The coupling constant λ can be related to Γ_γ , the rate of radiative N^* decay i.e. $N^* \rightarrow N + \gamma$. This follows in a straightforward fashion from (1). See Appendix.

$$\left(\frac{\lambda}{m}\right)^2 = 86 \pi \frac{M^5}{(M+m)^2} \frac{\Gamma_\gamma}{(M^2-m^2)^3} \quad (3)$$

The differential cross section for N^* Coulomb production can be expressed in terms of Γ_γ

$$\frac{d\sigma}{d\Omega} = 16 \pi^2 \alpha \left(\frac{M}{M^2-m^2}\right)^3 \Gamma_\gamma |F|^2 \frac{\sin^2 \theta}{\left[\left(2 \sin \frac{\theta}{2}\right)^2 + \left(\frac{M^2-m^2}{2 p_1^2}\right)^2\right]} \quad (4)$$

Here, θ is the laboratory angle between \vec{P} and \vec{p}_1 . The 4 momentum transfer to the nucleus is given by

$$-t = q^2 = p_1^2 \left[4 \sin^2 \frac{\theta}{2} + \left(\frac{M^2-m^2}{2 p_1^2} \right)^2 \right] \quad (5)$$

Since only very small angles θ are relevant we can write

$$\frac{d\sigma}{d\Omega} = 16 \pi^2 \alpha \cdot \left(\frac{M}{M^2-m^2}\right)^3 \Gamma_\gamma |F|^2 \frac{\theta^2}{\left[\theta^2 + \left(\frac{M^2-m^2}{2 p_1^2}\right)^2\right]^2} \quad (6)$$

- 3 -

Another useful variant of the cross section equation is

$$\frac{d\sigma}{dq^2} = 16\pi Z^2 \alpha \left(\frac{M}{M^2 - m^2} \right)^2 \Gamma^2 |F(q)|^2 \frac{(q^2 - q_{\min}^2)}{q^4} \quad (7)$$

The differential cross section can be modified to explicitly display the N^* mass dispersion by multiplying by a Breit-Wigner term. See Appendix.

A large degree of spin alignment is induced into the N^* . The angular distribution of the decay pion in the N^* C.M. is proportional to $(1 + 3/2 \sin^2 \theta_{\pi})$ where θ_{π} is the angle between the pion and N^* directions.

Let the factor $f(\theta)$ be defined as the last part of Equation 4, i.e.

$$f(\theta) = \frac{\sin^2 \theta}{\left[\Delta^2 + 1/4 \sin^2 \frac{\theta}{2} \right]^2} \quad (8)$$

where $\Delta \equiv \frac{M^2 - m^2}{2 p_1^2} = s_{\min}/p_1$.

In the limiting case of a point nucleus (achieved by using sufficiently high incident energies so that $q \sim$ small), $F(q^2) = 1$. The total cross section is then easily obtained by noting that

$$\int f(\theta) d\Omega = 2\pi \left[\left(\frac{1}{2} + \frac{\Delta^2}{4} \right) \log \left(1 + \frac{4}{\Delta^2} \right) - 1 \right] \quad (9)$$

As far as final charge states are concerned,

$$\begin{array}{ll} n + \gamma_0 \rightarrow \pi^- + p & (1/3) \\ n + \gamma_0 \rightarrow \pi^0 + n & (2/3) \\ p + \gamma_0 \rightarrow \pi^+ + n & (1/3) \\ p + \gamma_0 \rightarrow \pi^0 + p & (2/3) \end{array} \quad (10)$$

The analogous formula to Eq. 6 for bosons 4 describing e.g.

$$\pi^\pm + \gamma_0 \rightarrow \pi^\pm \text{ is}$$

$$\frac{d\sigma}{d\Omega} = 24\pi Z^2 \alpha \left(\frac{m_\pi}{m_p^2 - m_\pi^2} \right)^3 \Gamma_{\rho \rightarrow \pi\gamma}^2 |F|^2 \frac{e^2}{\left[e^2 + \left(\frac{m_\pi^2 - m_p^2}{2 p_1^2} \right)^2 \right]^2} \quad (11)$$

- 4 -

The corresponding ρ decay angular distribution is simply $\sin^2 \theta_\pi$.

Using the value $\Gamma_\gamma = 0.7 \text{ MeV}^5$ given by N^* photoproduction experiments and $|F| = 1$ we can numerically evaluate the cross section for Coulomb N^* production. See Table 1.

C. Nuclear Form Factor

The form factor $F(q^2)$ depends on two features, the nuclear charge distribution and the effect of absorption or scattering on those nucleons which have impact parameters \lesssim the nuclear radius. The former effect is reasonably well known from other measurements, principally electron scattering. The latter requires a knowledge or estimate of the complex forward scattering amplitude of the N^* in nuclear matter and cannot be regarded as well established. In principal, $F(q^2)$ could be modified by an optical model calculation which included both these features. If however, the measurements are restricted to small q^2 we can set $F(q^2) = 1$ to reasonably good approximation. This is equivalent to demanding that the great bulk of the N^* be produced outside the nucleus. This condition in turn is satisfied by requiring that the incident energy be sufficiently large.

In order to gain insight into the required nuclear energy and q restrictions, let us examine $f(\theta)$. We note that $f(0) = 0$, $f(\theta) \sim \theta^{-2}$ for $\Delta \ll \theta \ll 1$ and $f(\theta)$ has a maximum for $\theta = \Delta$. In order to get a reasonable experimental yield we would hope to have a cutoff θ of at least 2Δ . If θ is cutoff below Δ , the yield would be drastically reduced. A smaller nucleus would have a weaker q dependence in $F(q^2)$ but the Z^2 dependence of the effect suggests that nuclei smaller than Pb be used only for checking the theory or other special circumstances.

Note that the denominator of $f(\theta)$ contains q^4 the same factor encountered in the more familiar Rutherford elastic scattering formula. It is well known

- 5 -

that for this case, the small θ events correspond to classical particle trajectories which have large impact parameters. The same is more or less true in the present situation. The requirement of N^* production outside the nucleus (at least dominantly) demands $q \lesssim \hbar/R$ where R is the radius of the nucleus in question. For the case of Pb $\hbar/R \approx 30$ MeV/c and the minimum $q \approx 0.6$ (BeV)²/2p₁. Thus an incident beam with $p_1 \gtrsim 15$ BeV/c would be satisfactory.

D. Background Considerations

There are several reasons for using a heavy nucleus such as Pb. The most obvious one is the Z^2 dependence in Equation 4. Furthermore the largely incoherent nuclear cross section scales as $A^{2/3}$ which helps optimize the effect relative to background. One expects that these background processes will have reasonably high particle multiplicity which facilitates their rejection. The multiplicity scales roughly as $e^{1/4}$. By using a nucleus with a radius much larger than the nuclear mean free path for interaction, we expect to gain even further multiplicity. In fact, the core of a large nucleus is sufficiently absorptive as to make only the toroidal rim of a nucleus corresponding to near grazing impact parameters a relevant source of background. Thus relevant background scales very roughly as $A^{1/3}$.

It is probable that the largest source of background both in triggering and the ultimate kinematical separation, comes from channels where the nucleus also recoils coherently. The most important of these would appear to be $N + A \rightarrow N^*(1236) + A$ via ρ^0 exchange.⁶ The amplitude of this process should be proportional to $F(q) \sin \theta$ in contrast to the $F(q) \sin \theta/q^2$ factor in the N^* Coulomb process. Thus an interference term with softer maximum at a larger value of q^2 than the Coulomb process results. The presence of such a term could be tested experimentally by reducing Z . In fact, the

- 6 -

prospect for obtaining some additional physics data concerning ρ^0 exchange is encouraging.

In addition, the process $N + A \rightarrow N + \text{several } \pi\text{'s} + A$ is expected to occur via the exchange of the "Pomeron". The multipion events should be kinematically separable. Of particular interest however, is the production of the broad resonance $N^*(1470)$ which decays 55% of the time into $N\pi$. The tail of this state may interfere with the Coulomb production of $N^*(1236)$. The amplitude for $N^*(1470)$ production would be proportional to $F(q)$ so that the potential for complicating the small q^2 coherence pattern is somewhat greater than the ρ^0 exchange process. Nevertheless, variation of Z and examination of the $N\pi$ final state mass spectra should provide separation. Again, we regard such a feature as interesting rather than debilitating.

We have already noted that a substantial part of the nuclear interactions will be characterized by large particle multiplicity. A further possibility for trigger background suppression is provided by the fact that the final nuclear system is in general, highly excited. A large multiplicity of MeV evaporation nucleons and γ -rays will be emitted in a roughly isotropic fashion. In a counter-spark chamber experiment veto counters can be positioned about the target to cover all but small entrance and exit holes and suppress these unwanted interactions. It is difficult to predict quantitatively the efficacy of this suppression. It is probably easier to measure it.⁷

We conclude these considerations on a positive note by observing that the useful yield of the Coulomb production process increases with incident energy³ while all background channels are progressively easier to separate. The final conclusive separation of the effect depends on the kinematical reconstruction of the events and the observation of the sharp coherent angular distribution described by $f(\theta)$.

E. Applications

As we have seen, the Coulomb N^* production from Pb and presumably the ρ , K^* , Y^* and antiparticle analogies as well, have a useful cross section of a few mb, (for $p_L > 20$ BeV/c) to be compared with a total interaction cross section of 2.0 b. The highly directional character of this process is compatible with large detection efficiency. In fact, the magnitude of the effect is reminiscent of and compares favorably with the process of coherent K_S^0 regeneration. The ratio of regenerated K_S^0 emerging from a thick slab to incident K_L^0 is usually a few parts per ten thousand.

The geometry of a counter spark chamber experiment to detect $n + \gamma_C \rightarrow N^{*0} \rightarrow \pi^- + p$ is remarkably similar to that of a K_S^0 regeneration experiment. The analyzing magnet requirements in so far as aperture and analyzing power are concerned are about the same. The principal difference is that the N^{*0} "V" originates in the target slab. A reasonable choice of target would be a 0.6 cm sheet of Pb which equals about one radiation length and 10% of an interaction length. The mean multiple Coulomb scattering induced transverse momentum smearing imparted to the emerging proton and π^- would be about 15 MeV/c. This would not mask the characteristic sharp angular definition of the process.

A spectrometer may be constructed with wire spark chambers and magnet for detecting neutrons with good energy resolution. Event rates in excess of 10/machine pulse seem reasonable. The largest uncertainty, noted previously, is in connection with background rejection in triggering. If trigger blocking occurs or if it becomes necessary to apply some kinematical constraints in triggering, e.g. requiring the π^- and p to have approximately equal and opposite transverse momentum, some reduction in yield would result. Nonetheless, the prospects for having enough rate to execute precision

neutron transmission experiments appear promising.⁹ The useful detection of scattered neutrons is more problematic and will not be discussed.

Let us consider the process $p + \gamma_C \rightarrow N^{*+} \rightarrow \pi^+ + n$. Well focused high energy, monochromatic proton beams of almost arbitrary flux are available. The above process should be discernable by a measurement of the π^+ momentum and the direction of the neutron. Typically, the π^+ momentum will be $\sim 25\%$ of the beam momentum. Since N^{*+} photoproduction experiments have been carried out, the observation of the Coulomb N^{*+} production would provide a very powerful check on the correctness of our ideas and approximations, particularly pertaining to nuclear coherent background. Indeed, our confidence in the Primakoff method determination of the π^0 and η^0 lifetime could be tested. Because of the good focusing properties of the proton beam, the transverse dimensions of the Pb target and the associated incoherent background rejecting counter array would be small. The triggering could be readily tested.

The above process could provide a tagged neutron beam. By tagged we mean in time coincidence with the incident proton and with neutron momentum accurately given by the difference of the incident proton and π^+ momenta. Neutron measurements have been performed and are proposed, using total absorption arrays or "calorimeters" constructed of scintillator and heavy material such as Fe. These have the features of high efficiency (near 100%) and relatively poor energy resolution. At the very least, it would appear useful to use the tagged neutron scheme to calibrate experimentally the properties of such instruments.

A small angle n-p charge exchange study could be carried out using this tagged beam. Such measurements have been carried out in the past using neutrons initially produced by elastic charge exchange. This is an intrinsically

incoherent process. The tagged neutron scheme has better prospects for very high energies. Some secondary advantages are worth noting. The tagged neutron scheme will provide data for a range of neutron momenta. The elastic charge exchange mode of production requires a variation of proton beam momenta which may be inconvenient at a major multiple use accelerator. The tagged neutron process also provides the possibility of a good absolute normalization.

The diffractive dissociation process $p + A \rightarrow N^{*+}(1470) \rightarrow n + \pi^+$ may provide an alternate or supplementary basis for tagged neutron work. Nuclear reabsorption considerations might then suggest the use of a lower Z target such as Aluminum. A rough estimate indicates that this cross section is ~ 2 mb/Pb nucleus at a proton beam energy ~ 25 BeV/c.¹³

Some magnet spark chamber arrays have been designed to work in a bubble chamber like fashion i.e. measure events of complex topology with high detection efficiency but with modest incident flux requirements. Tagged neutrons and perhaps even tagged antineutrons may be useful.

In summary, the availability of beams of increasing energy and diversity makes the use of the nuclear Coulomb field as an interaction target an increasingly attractive prospect.

Footnotes and References

1. H. Primakoff, Phys. Rev. 81, 899 (1951).
 G. Chiuderi and G. Morpurgo, Nuovo Cimento 19, 497 (1961).
 C. A. Englebrecht, Phys. Rev. 133, 988 (1964).
 V. Glaser and R. A. Ferrell, Phys. Rev. 121, 886 (1961)
2. M. Good and W. Walker, Phys. Rev. 120, 1855 (1960).
3. I. Pomeranchuk and I. Shmushkevich, Nucl. Phys., 23, 452 (1961).
4. S. M. Berman and S. D. Drell, Phys. Rev. 133, 791 (1964).
5. The calculations follow the technique and notation described in "Cross Section and Form Factor of $N^*(1236)$ Production by Electrons", Y. Nagashima, University of Rochester Report, UR-875-189 (unpublished).
6. Reference 4 contains a rough estimate of the process $\pi^{\pm} + A \rightarrow \rho^{\pm} + A$ via ω^0 exchange. It is concluded that for sufficiently large incident energies that this background is not prohibitive. Essentially the same considerations carry over to the $N^*(1236)$ production by ρ^0 exchange. But note that the ρ^0 exchange contributions from the neutrons and the protons have opposite sign so that there is a large degree of cancellation. A more detailed consideration of ρ exchange using the optical model program of G. Morpurgo is given in a GEM proposal for a measurement of $K + \gamma_C \rightarrow K^* + C.E.R.N., E.T.H., Imperial College Collaboration (C. Bemporad et al.) P.H.I./COM 68 - 19$. We thank Professor A. Melissinos for bringing this work to our attention.
7. Experiments using K^{\pm} charge exchange in complex nuclei have been carried out by many groups including one from Rochester. The $K^0(\bar{K}^0)$ yields quoted are usually substantially lower than hydrogen or deuterium data would predict. This is because this incoherent process is accompanied by nuclear excitation which is inadvertently detected by

veto counters. Some Rochester measurements (unpublished) relevant to the question of incoherence rejection are generally encouraging.

8. We have considered the Coulomb production process only in first order. The quantity $Z^2\alpha$ is not particularly small however, and higher order corrections may become important at the higher energies where the cross section is large. Intuitively, we expect that there will be a few percent reduction in yield. This should result from the attenuation of the N^* in the Coulomb field, primarily by inducing a transition back to the nucleon state. Bremsstrahlung by either the incident nucleon or outgoing N^* may be significant. There may even be some magnetic reorientation of the N^* spin alignment axis. A correction which had some sensitivity to the N^* magnetic moment would be interesting. A treatment of these higher order effects should be thorough and comprehensive and we are not prepared to pursue the matter in this paper.
9. A precision measurement of the energy dependent n p total cross section is one obvious application. Cross sections for deuterium and other nuclei are of interest also. See the discussion on inelastic shadow effects in nuclear cross sections, J. Pumplin and M. Ross, Phys. Rev. Letters 21, 1778 (1968).
10. C. Becchi and G. Morpurgo, Phys. Rev. 140, B 687 (1965).
11. W. Rarita and J. Schwinger, Phys. Rev. 111, 329 (1958).
12. L. Stodolsky, Phys. Rev. 134, B 1099 (1964).
13. This rough estimate is primarily based on an extrapolation from the work of F. R. Huse et al., Nucl. Phys. B 8, 391 (1968). They measure the cross section for coherent $p + \text{Neon} \rightarrow \text{Neon} + p \pi^+ \pi^-$ (1470) to be $470 \pm 100 \mu\text{b}$. We make "reasonable" assumptions about the $p \pi^+ \pi^-$ and $n \pi^0$ branching fractions and scale to the case of Pb. This scaling depends strongly on the large self absorption effect in Pb. We roughly infer

this from data on coherent photo ρ^0 production experiments (F. Lobjewicz private communication).

14. Elementary Particle Physics, G. Källén, Addison-Wesley, Chapter 6.

- 13 -

Table 1

p(BeV/c)	$N + \gamma_C \rightarrow N^*$		$\pi^\pm + \gamma_C \rightarrow \rho^\pm$	
	$q_{\min}(\text{MeV/c})$	$\sigma'(\text{mb})$	$q_{\min}(\text{MeV/c})$	$\sigma'(\text{mb})$
15	20.5	1.05	18.6	0.11
20	16.1	2.4	14.0	0.335
25	13.0	4.0	11.2	0.51
50	6.47	9.75	5.6	1.05
100	3.23	15.8	2.8	1.65
200	1.61	22.2	1.4	2.25

The quantity $\sigma' \equiv \int_{q_{\min}}^{q_1} (d\sigma/dq^2) dq^2$ has been evaluated for both N^* and ρ production using $\frac{q_{\min}}{5} = 32$ and $q_1 = 30$ MeV/c. This value of q_1 is consistent with the approximation $|F| = 1$. Recall that $[F(q) - 1] \approx \frac{q^2 \langle r^2 \rangle_{av}}{6}$. The value $\Gamma_\gamma = 0.7 \text{ MeV}^5$ given by N^* photoproduction experiments and the theoretical prediction $\Gamma_{\rho^+ \pi^+ \gamma} = 0.120 \text{ MeV}^{10}$ have been used.

APPENDIX

To calculate the cross-section, we follow the formalism developed by Rarita and Schwinger ⁽¹¹⁾ regarding N^* (1236) to be a spin $3/2^+$ elementary particle. The finite width of N^* will be taken into account later. According to them a spin $3/2$ object is described by a vector spinor field Ψ_μ which satisfies the equation of motion

$$(\gamma_\nu \partial_\nu + M) \Psi_\mu = 0 \quad (A-1)$$

with the subsidiary condition

$$\partial_\mu \Psi_\mu = 0 \quad (A-2)$$

The propagator of the particle is written in the form

$$\begin{aligned} S_{F\mu\nu} &= \frac{M-i\hat{p}}{M^2 - p^2} \left\{ S_{\mu\nu} - \frac{1}{3} \gamma_\mu \gamma_\nu - \frac{i}{3M} (\gamma_\mu \hat{p}_\nu - \gamma_\nu \hat{p}_\mu) + \frac{2}{3M^2} \hat{p}_\mu \hat{p}_\nu \right\} \\ &\equiv \frac{\Lambda_{\mu\nu}}{M^2 - p^2} \end{aligned} \quad (A-3)$$

The projection operator to the positive energy state is given by

$$\sum_{\text{spin}} u_\mu(p) \bar{u}_\nu(p) = \frac{\Lambda_{\mu\nu}}{2M} \quad (A-4)$$

Under the assumption of the pure magnetic dipole transition for the process

$$\gamma + N \rightarrow N^*, \quad \text{the relevant matrix element is } (12)$$

$$\begin{aligned} A_\mu(q) &\langle P | J_\mu(0) | N \rangle \\ &= \left(\frac{M+m}{E} \right)^{\frac{1}{2}} \frac{\lambda(q)}{m} A_\mu(q) \varepsilon_{\mu\nu\rho\sigma} \bar{u}_\nu(p) u(p) \frac{p_\sigma}{M} \gamma_\rho \end{aligned} \quad (A-5)$$

Where q is the 4-momentum of the photon (real or virtual).

The S-matrix element for the process N^* decaying into $N + \gamma$ is given by

$$S_{fi} = -(2\pi)^4 i \delta^4(P - q - p) \frac{e_{\mu}^{\alpha}}{\sqrt{2} q_0} \langle N | J_{\mu}(0) | N^* \rangle \quad (A-6)$$

where e_{μ}^{α} is the polarization vector of the photon.

$$\begin{aligned} \Gamma_{\gamma} &= \text{(Total decay probability of } N^* \rightarrow N + \gamma \text{)} \\ &= \frac{1}{4} \sum_{\text{spin}} \int |S_{fi}|^2 \frac{d^3 p}{(2\pi)^3} \frac{d^3 q}{(2\pi)^3} \end{aligned} \quad (A-7)$$

Using (A-6) we obtain after straight-forward calculation

$$\Gamma_{\gamma} = \frac{1}{768\pi} \left(\frac{\lambda}{M} \right)^2 \frac{(M+m)^2 (M^2 - m^2)^3}{M^5} \quad (A-8)$$

The photoproduction cross-section of N^* can be obtained using the same S-matrix element.

$$\sigma_{\gamma} = \frac{1}{4v} \sum_{\text{spin}} \int |S_{fi}|^2 \frac{d^3 p}{(2\pi)^3} = \frac{4\pi^2}{q^{*2}} M \Gamma_{\gamma} \delta(P^2 - M^2) \quad (A-9)$$

Here q^{*2} is the momentum of the photon in N^* CM system and is given by

$$q^{*2} = \frac{M^2 - m^2}{2M} \quad (A-10)$$

The equation (A-9) can be modified to include the finite width of the N^* .

We simply replace the δ function by the Breit-Wigner term

$$g(M) = \frac{1}{\pi} \frac{M_0 \Gamma}{(M^2 - M_0^2)^2 + (M_0 \Gamma)^2} \quad (\text{A-11})$$

Then the photoproduction cross-section of N^* takes the more familiar form

$$\sigma_{\gamma} = \frac{4\pi}{q^2} \frac{M_0^2 \Gamma^2}{(M^2 - M_0^2)^2 + (M_0 \Gamma)^2} \quad (\text{A-12})$$

Now to obtain the N^* production cross-section by the nuclear Coulomb field, we regard A_{μ} as the external field and put

$$A_{\mu}(q) = (0, 0, 0, i \mathbb{R}_2 F(q^2)/q^2) \quad (\text{A-13})$$

in the laboratory system. Utilizing the same manipulation as before, we get

$$\begin{aligned} d\sigma(\pi^0 + \gamma \rightarrow N^*) &= \frac{2\pi}{q^2} \int d\Omega \frac{1}{2} \sum_{\lambda} |K_{\lambda}(q)|^2 \frac{F^2(q^2)}{(q^2)^2} \frac{d^3 p}{(2\pi)^3} \\ &= \frac{1}{2} \frac{4\pi}{q^2} \frac{F^2(q^2)}{(q^2)^2} \int d\Omega \frac{d^3 p}{(2\pi)^3} \quad (\text{A-14}) \end{aligned}$$

which becomes in the small momentum transfer limit

$$\frac{d\sigma}{d\Omega} = \frac{1}{2} \frac{4\pi}{q^2} \frac{F^2(q^2)}{(q^2)^2} \frac{d^3 p}{(2\pi)^3} \quad (\text{A-15})$$

The alternative expression can be obtained by using the eqs. (A-9) and (A-10)

$$\frac{d\sigma}{dM^2 d\Omega} = \frac{2\pi}{q^2} \frac{F^2(q^2)}{(M^2 - m^2)^2} \frac{d^3 p}{(2\pi)^3} \quad (\text{A-16})$$

The assumption of a purely magnetic dipole transition matrix element implies the "well known" decay angular distribution¹⁴

$$W(\theta_{c.m.}) = \frac{1}{2} \left(1 + \frac{3}{2} \sin^2 \theta_{c.m.} \right) \quad (\text{A-17})$$

where $\theta_{c.m.}$ is the angle between the decay pion and the N^* direction in the N^* center of mass.

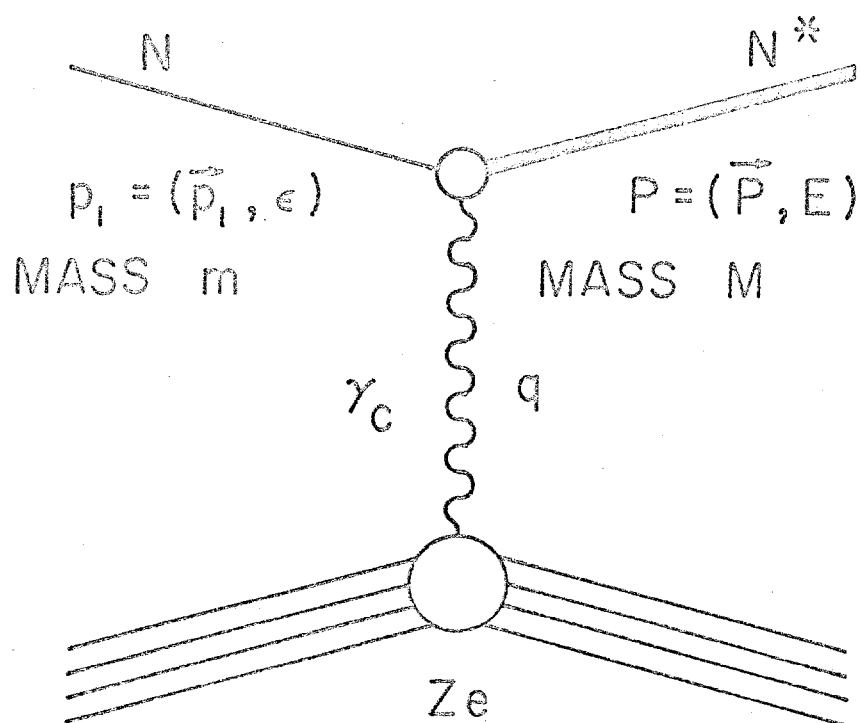


Figure 1

Coherent Production of N^* by N in the Coulomb Field of a
Nucleus of Charge Ze

PROPOSAL TO STUDY THE COHERENT DISSOCIATION
OF NEUTRONS

T. Ferbel, B. Gobbi, J. Rosen, S. Shapiro, P. Slattery
and B. Werner, University of Rochester, E. J. Bleser,
National Accelerator Laboratory, S. L. Meyer and D. H.
Miller, Northwestern University

Correspondent: J. Rosen
Department of Physics
University of Rochester

ABSTRACT

At NAL energies, neutrons can be coherently excited by nuclei with appreciable cross section. By coherent we mean that the target nucleus recoils as a single entity without nuclear excitation. This neutron excitation can occur either by γ absorption in the nuclear Coulomb field (Coulomb dissociation) or by Pomeron exchange in the nucleus (diffractive dissociation). Both channels can result in the formation of π^-p V's. We propose to study such V's using a spectrometer consisting of wire spark chambers, counters and analyzing magnet.

The two coherent processes can be identified and distinguished by their characteristic variation with neutron energy, momentum transfer, angular correlation, effective mass and A dependence. The former process (Coulomb) is dominated by $\Delta^0(1236)$ production while the latter is dominated by $N^*(1470)$ production. Coulomb dissociation is expected to be an order of magnitude more copious in high Z materials.

The objectives of the experiment are:

- 1) High statistics, comprehensive study of Coulomb and diffractive dissociation. Variations in momentum transfer, angular correlations and invariant mass (up to ~ 3 GeV) will be investigated as a function of target material and neutron energy (50-200 GeV).
- 2) Observe Coulomb and diffractive dissociation of the anti-neutron.

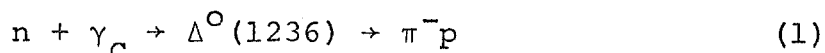
- 3) Survey the neutron and anti-neutron flux in the neutral beam.
- 4) Using transmission targets, measure neutron total cross sections as a function of energy.

I. Physics Justification

1) Coulomb Dissociation

The possibility that an elementary particle can be excited into a different state as a result of its interaction with the Coulomb field of a target nucleus was explored initially by Primakoff.⁽¹⁾ Subsequent calculations⁽²⁾ have elaborated on the rich physics consequences of this idea. In particular, Nagashima and Rosen⁽²⁾ have stressed that the Coulomb production of the $\Delta(1236)$, a process which can be calculated to great accuracy, can (1.) be used to test our understanding of the Primakoff process and thereby lend credence to the assumptions underlying our present knowledge of the π^0 and η^0 lifetimes, and (2.) be used to provide an efficient neutron detection scheme with excellent energy and directional properties.

The Coulomb production of $\Delta^0(1236)$ can be calculated in a rather straightforward manner.⁽²⁾ The differential cross section for the reaction:



where γ_C refers to the photon from the nuclear Coulomb field of a high Z target material, is given by⁽³⁾:

$$\frac{d\sigma}{dt} = \frac{16\pi}{3} Z^2 \alpha \left(\frac{M}{M^2 - m^2} \right)^3 \Gamma_\gamma |F(t)|^2 \frac{(t - t_{\min})}{t^2} \quad (2)$$

where M and m are masses of the $\Delta(1236)$ and the neutron respectively, Γ_γ is the known radiative width of the Δ , $F(t)$ is the nuclear form factor, α the fine-structure constant, and

Z is the nuclear charge. The integrated cross section for reaction (1) is rather substantial at present accelerator energies and, most importantly, grows significantly with increasing energy (essentially due to kinematic effects of t_{\min}). At 200 GeV/c, for example, approximately 0.5% ($\approx 7\text{mb}$) of the total interaction cross section for neutrons on Pb can be attributed to reaction (1). From expression (2) it is apparent that the natural width of the t -distribution in reaction (1) is typically of the order of t_{\min} . For 200 GeV/c neutron momentum, $\sqrt{t_{\min}} \approx \frac{M^2 - m^2}{2p} \approx 2 \text{ MeV/c}$. Thus the Coulomb peak is very sharp and its measured width will be determined by our apparatus which is capable of measuring transverse momenta with a sensitivity of $\lesssim 10 \text{ MeV/c}$.

2) Diffraction Dissociation

The nuclear diffraction dissociation phenomenon has been discussed extensively over the past few years⁽⁴⁾; and although several good experiments have been performed to study this process⁽⁵⁾, many quantitative questions regarding, for example, the amount of resonant contribution present in the dissociated system, the detailed nature of the energy dependence, and the phase of the diffraction dissociation amplitude, are still unanswered. The precise investigation of inelastic diffraction production processes, processes which are responsible for a large fraction of the observed total cross section in hadronic collisions, is clearly an important prerequisite to the understanding of strong interactions in general.

The differential cross section for neutron dissociation can be written as follows:

$$\frac{d\sigma}{dt} = \frac{d\sigma}{dt}_N A_{\text{eff}}^2 |F(t)|^2 \quad (3)$$

where $\frac{d\sigma}{dt}_N$ is the differential cross section for diffraction production (via $I = 0$ exchange without spin-flip) off a free nucleon, and A_{eff} can be regarded as the effective number of nucleons which take part in the coherent process ($A_{\text{eff}} \ll A$ for large nuclei because of the severe damping which hadrons experience in transversing nuclear matter. We estimate that for $N^*(1470)$ coherent production, for example, A_{eff} for C is ~ 5 , while for Pb it is ~ 15 .) The form factor of the nucleus can be parameterized in terms of the r.m.s. radius R :

$$|F(t)|^2 = e^{-\frac{R^2}{3}t} \quad (4)$$

with $R \sim 1.1 A^{1/3}$ fermi. Thus, the typical momentum transfer involved in the coherent diffractive dissociation of the neutron is $\sim (10 + 10A^{2/3})^{-1/2}$ GeV/c. For a Pb nucleus this corresponds to a transverse momentum of ~ 50 MeV/c, a momentum whose measurement is well within the resolution capability of our apparatus. For lighter nuclei, the typical transverse momenta in the diffraction dissociation process will be somewhat larger (for C it is ~ 140 MeV/c).

At NAL energies, the Coulomb production of $\Delta^0(1236)$ in high-Z materials dominates neutron diffraction dissociation (e.g., into the $N^*(1470)$ object), while the opposite is the

case for low-Z elements (see Fig. 1). Both processes are copious and both are characterized by an exceedingly steep t-dependence. In the case of the Coulomb process the inherent width of the forward momentum-transfer peak is determined essentially by the value of t_{\min} (not sensitive to the nuclear shape - $|F(t)|^2 \sim |F(0)|^2 \sim 1.0$), while the momentum transfer dependence in neutron diffraction dissociation has the width characteristic of the nuclear target radius. Figure 2 displays the relative shapes expected for the t-spectra for neutron dissociation (Coulomb and diffractive) off a medium-size nucleus, such as Cu. The width of the peak for the forward production of $\Delta^0(1236)$ has been broadened to account for experimental resolution.

It appears that the dissociation of a neutron into a $p\pi^-$ system, at the high energies available at NAL, will be a particularly tractable way to probe the nature of both the Coulomb dissociation and the nuclear diffraction dissociation phenomenon. A neutron which converts into a $p\pi^-$ "V" within a complex nucleus can readily be identified through the use of rather standard V-spectrometer detection systems (details described later). With an expected transverse momentum resolution of ~ 10 MeV/c, the kinematic separation of the $p\pi^-$ dissociation events from the background should prove to be a relatively easy task.

3) Survey of Neutron and Anti-Neutron Flux in the Neutral Beam.

An examination of Fig. 1 clearly reveals the previously noted fact that the $\Delta^0(1236)$ Coulomb production cross section in Pb is quite substantial. This suggests the possibility of using the $\Delta^0(1236)$ production mechanism in Pb as a reasonably efficient tool for neutron detection. The neutron and anti-neutron flux in the small angle neutral beam at NAL can be surveyed using a $\sim \frac{1}{4}$ radiation length Pb target (this is only $\sim \frac{1}{100}$ of an interaction mean free path). With a flux of $\sim 10^7$ neutrons/pulse we expect on the average a useful neutron conversion yield of ~ 100 counts/pulse. This rate is more than adequate for the neutron flux measurements, and should be sufficient to provide good data on the anti-neutron flux - particularly at lower energies (50 GeV) where the yield might be several percent of the neutron flux. The excited anti-neutron dissociates to an anti-proton and a π^+ and can be easily distinguished kinematically from the neutron dissociation.

4) Neutron Total Cross Section

By placing transmission targets in the beam far upstream of our V-spectrometer we plan to obtain better than 1% measurements of neutron total cross sections on hydrogen and on complex nuclei in 5 GeV/c momentum bands for the neutrons in the energy range between 50 GeV/c and 200 GeV/c. The anti-neutron measurements and a K_L^0 survey will be used to correct these precision cross sections.

The K_L^0 component of the neutral beam will be assayed through the measurement of the leptonic decays $K_L^0 \rightarrow \pi^\pm \mu^\pm \nu$. This can be achieved during one day of running time (the modification to the apparatus involves only minor changes).

The program involving the neutron studies described in the preceding pages is to be carried out in ~600 hours of data taking.

II. Experimental Equipment

The principal items which are required for the execution of this experiment are indicated schematically in Fig. 3. We will briefly describe these, and several other items of importance, in the order outlined below:

1. Neutral beam
2. Target and Target Counter System
3. Vertex Chamber
4. Gas Cerenkov Counter
5. Wide Aperture Magnet
6. Trigger Hodoscopes
7. Wire Spark Chambers
8. Dedicated Computer

1. Neutral Beam

A well-collimated, small-angle neutral beam is required. A flux of 10^7 neutrons in the momentum range of 50 GeV/c to 200 GeV/c, having a beam cross section of about 1-2 (inch)² at

1500' from the production target is suitable.

2. Target, Target Counter System

For the study of the coherent nuclear and Coulomb dissociation reactions, we propose to use $1/4$ radiation length targets. Our minimum program will involve detailed investigations using Pb, Cu, Al, and C. These will be sandwiched between a $1/16$ " thick veto and a $1/32$ " thick trigger counter.

The target will be surrounded on all sides, except for entrance and exit holes on the beam axis, with a veto complex which will serve to suppress uninteresting nuclear reactions (large particle multiplicity or nuclear fragmentation). A schematic layout of the veto complex, which will shortly be used in a similar experiment at the AGS,⁽⁶⁾ is shown in Fig. 4. This arrangement has been constructed and was tested successfully at the AGS this past year. (In fact, it was on loan to Dr. Finocchiaro (SUNY) who used it in a diffractive scattering experiment carried out in a high flux π^- beam.)

For hydrogen and deuterium total cross section measurements we require a transmission target of (10-20)g thickness, located in the neutron tunnel. A cryogenic target - (4-8)' x 3" diameter would be adequate. A much simpler alternative is the use of a high pressure gas target. At normal storage cylinder pressure (2000lbs.) the target would have to be $\sim(20-40)$ ' long. It would be formed in several sections.

3. Vertex Chambers

Following the target complex we will place a set of high-resolution (<0.5 mm), horizontal and vertical, multiwire

proportional chambers. These will establish the initial transverse vertex coordinates of the V. They will present less than 50 mg of interaction material to the high-flux neutron beam. Approximately 200 wires will be involved. Testing of efficiency, stability, and reliability of the system is now underway in the laboratory and in a test beam at the AGS. The results have thus far been completely satisfactory.

4. Gas Cerenkov Counter

The bulk of the upstream region will be filled with a 15 meter 1 atmosphere threshold Cerenkov counter. The basic gas fill will be hydrogen. A $\beta = 1$ particle will provide 200 photons under these conditions and the Cerenkov angle will be 1° . The threshold energies will be 57, 30, 8.4 GeV for protons, kaons, and pions respectively. The total thickness of the hydrogen gas will be 0.15 g.

The counter will have thin mylar windows and a 45° stretched aluminized mylar mirror to reflect the light vertically where a hodoscope of photomultipliers and light gathering reflectors will be positioned.

It is proposed that this counter be constructed at NAL under the supervision of Drs. Bleser and Rosen. The cost should be under \$10K.

5. Wide Aperture Magnet

A 48D48 magnet will be suitable for the purposes of the present experimental design. With a gap of 18 inches, and an integrated field of 20 kG.m, this magnet will provide an

adequate transverse momentum kick of 0.6 GeV/c. Such a magnet costs approximately \$100K.

This magnet defines the limiting acceptance aperture, $\pm 9''$ (V), $\pm 24''$ (H). The corresponding acceptance for the magnet positioned at 17m from the target is ± 13 mrad (V) and ± 35 mrad (H).

6. Trigger Hodoscope

We will require 2 and only 2 charged particles passing through the system. This can be achieved through a rather straightforward triggering arrangement. The hodoscope information should also prove to be valuable in the pattern recognition of the wire spark chamber data.

7. Wire Spark Chambers

We have already constructed one of the multiple plane systems and are presently testing it (the chambers have useful areas of 46" x 92").

We wish to point out that we have extensive experience with this technique. We recently completed an experiment which recorded five million triggers and employed 12 wire planes. The chambers were completely fabricated in Rochester. (We are equipped to wind chambers of arbitrary size.) Data were produced with the aid of the Rochester-owned Honeywell DDP-516 computer and ancillary magnetostrictive equipment.

8. Dedicated Computer

The Rochester Group has recently purchased a PDP-15 system (now delivered) which will be available for this experiment. We request a link to a large time-sharing central

computer for selective on-line analysis. If this is not available, then off-line fast turn-around on a large NAL computer (\sim PDP-10) will be required.

III. Technical Details

1. Yields and Detection Efficiency

The envisioned neutron dissociation studies on C, Al, Cu and Pb, as well as the flux and total cross section measurements, will have substantial event rates. For the flux measurements, for example, we plan to use a 1.5 gm/cm^2 Pb target. As noted previously, the useful cross section for the Coulomb process (reaction 1), in the 50 GeV/c to 200 GeV/c momentum range, is about 5 mb/Pb nucleus. This gives an event rate of $\sim 300 \text{ p}\pi^-/\text{pulse}$. The detection efficiency of the $\text{p}\pi^- \text{ V}$ is largely determined by the solid angle acceptance of the magnet. These efficiencies have been evaluated with standard Monte Carlo techniques and are shown in Fig. 5. On the whole, the acceptance is large, and, in particular, for the Coulomb-produced $\Delta^0(1236)$ the efficiency will be $\sim 50\%$ for the entire neutron momentum range. The estimated yield of ~ 100 useful V's per 10^7 neutrons (one pulse) is sufficiently large for the precision measurement of neutron total cross sections and for a less accurate determination of anti-neutron cross sections.

2. Background

Although the useful yield of high energy $\pi^- \text{ p}$ pairs from the Coulomb process is $\sim 5 \text{ mb}$, it must be noted that the Pb interaction cross section is approximately geometric, i.e.,

~ 1500 mb. Now the great bulk of this cross section results in very large multiplicity and nuclear fragmentation events. In our background estimates we conservatively estimate that only the outer rim of ~ 500 mb projected area can be regarded as hydrogen-like, i.e., free of secondary interactions, reabsorption and remultiplication. (At A.G.S. energies it is observed that pp collisions result in single energetic $N\pi$ pairs for less than 1% of the interactions). Thus we expect trigger background from the nuclear rim with an effective cross section of a few mb or less. The incoherent background will cause no trouble in the analysis of the dissociation data since the t-spectrum from these events will be considerably flatter than from coherent interactions (see Fig. 2). Direct experimental data bearing on this point will be available shortly from the A.G.S. experiment. (5)

3. Resolution

The final kinematical analysis will involve the wire chamber measurement of π^- and p momenta. The coherent events will be signaturred by a sharp peak on a plot of events versus transverse momentum transfer. The sharp peak will be largely contained inside $q(\text{transverse}) \sim 100$ MeV/c. Incoherent background will have an average $q(\text{transverse}) \sim 300$ MeV/c. The expected angular resolution is $\sim 1 \text{ mm}/20\text{m} = 5.0 \times 10^{-5}$ rad, while the momentum resolution will be $\sim 1\%$. A 100 BeV/c proton, for example, will bend by $(0.6 \text{ BeV/c}/100 \text{ BeV/c}) = 6 \text{ mrad}$. This gives $\delta p/p = \delta \theta/\theta \sim 1\%$.

The uncertainty in $p(\text{transverse})$ resulting from angle uncertainty will be $p \delta\theta \sim 5 \text{ MeV/c}$. The actual limit on transverse momentum resolution comes from multiple Coulomb scattering, principally in the $1/4$ radiation length target. There are two particles produced on the average $1/2$ of the way into the target. Therefore, the uncertainty in the transverse momentum produced by the target is $\sim 10 \text{ MeV/c}$. Thus we see that the transverse resolution is adequate for resolving the sharp coherent spike.

The N^{*0} mass resolution is excellent. This can be inferred from the formula for the mass

$$\begin{aligned} m_{N^*}^2 - (m_p^2 + m_\pi^2) &= 2(E_p E_\pi - \vec{p}_p \cdot \vec{p}_\pi) \\ &= p_\pi p_p \left(\frac{m_\pi^2}{p_\pi^2} + \frac{m_p^2}{p_p^2} + \theta^2 \right) \end{aligned}$$

where $\theta = V$ opening angle. It is readily shown that

$\delta m_{N^*}/m_{N^*} \sim 1\%$, using the previously noted uncertainties on angle and momentum measurements.

It is interesting to note that this high mass resolution is achieved with a relatively small $\int B \, dl$. The opening angle of the V plays the crucial role. This is in sharp contrast with missing mass work for example, where the mass measurement depends on the differences in the momenta of incoming and outgoing particles.

Our analysis of the efficiency, resolution and separation of the aggregate coherent events should be regarded as proceeding along well established lines. Precisely the same considerations have been employed in successful experiments on

(a) coherent K_S^0 regeneration, and (b) diffractive ρ^0 production in photon beams. Both types of experiments study $\pi^+\pi^-$ V's produced in beams with wide band primary momentum distributions. Our yields per incident particle compare quite favorably with these experiments.

References

1. H. Primakoff, Phys. Rev. 81, 899 (1951).
2. M. Good and W. Walker, Phys. Rev. 120, 1855 (1960);
C. Chiuderi and G. Morpurgo, Nuovo Cimento 19, 497 (1961);
V. Glaser and R. A. Ferrell, Phys. Rev. 121, 886 (1961);
I. Pomeranchuk and I. Shmushkevich, Nucl. Phys. 23, 452
(1961); S. M. Berman and S. D. Drell, Phys. Rev. 133,
791 (1964); C. A. Englebrecht, Phys. Rev. 133, 988 (1964);
A. Halprin, C. M. Anderson, H. Primakoff, Phys. Rev. 152,
1295 (1966); Y. Nagashima and J. Rosen, University of
Rochester Report UR-875-295 (1969).
3. See the report of Nagashima and Rosen for details.
4. M. Good and W. Walker, Phys. Rev. 120, 1857 (1960); I. Pomeran-
chuk and I. Shmushkevich, op. cit.; M. Ross and Y.Y. Yam, Phys.
Rev. Letts. 19, 546 (1967); E. L. Berger, Phys. Rev. Letts.
21, 701 (1968); G. Chew and A. Pignotti, Phys. Rev. Letts.
20, 1078 (1968); also see report by H. H. Gingham, loc cit
for other references.
5. A. M. Cnops et.al., Phys. Rev. Letts. 25, 1132 (1970), and
references cited therein; C. Bemporad et.al., CERN preprint
(Kiev Conference-1970); R. Huson et.al., Nucl. Phys. B8,
391 (1968); Also see recent review paper by H. H. Bingham,
CERN Report D.Ph.II/PHYS/70-60.
6. An experiment on $\pi^- + \gamma_c \rightarrow \rho^-$ and $p + \gamma_c \rightarrow \Delta^+$ is scheduled to
begin this spring at the A.G.S. The Rochester group will
carry out this experiment using the Lindenbaum-Ozaki
spectrometer. Triggering tests, which have relevance to

References continued

the present proposal, were satisfactorily completed during the summer of 1970. Using an 8 BeV/c π^- beam and a simulated triggering arrangement, including the target veto counter complex, we looked for ρ^- -like triggers originating from 1/4 radiation targets of Pb, Cu, and Al. Our expectations concerning incoherent trigger background were confirmed. Detailed results will be provided upon request.

Figure Captions

Fig. 1. Z dependence of the dissociation cross sections at 100 GeV/c for the reactions $n + \gamma_c \rightarrow \Delta^0(1236) \rightarrow p\pi^-$ and $n + A \rightarrow N^*(1470) + A \rightarrow p\pi^- + A$.

Fig. 2. Expected relative shape for the t-spectra for neutron dissociation (Coulomb and diffractive) off Cu.

Fig. 3. The proposed experimental layout.

Fig. 4. Target arrangement.

Fig. 5. Spectrometer acceptance. The percentage of N^* decays accepted by the V-spectrometer as a function of N^* mass for initial neutron momenta of 50, 100, 150 and 200 GeV/c.

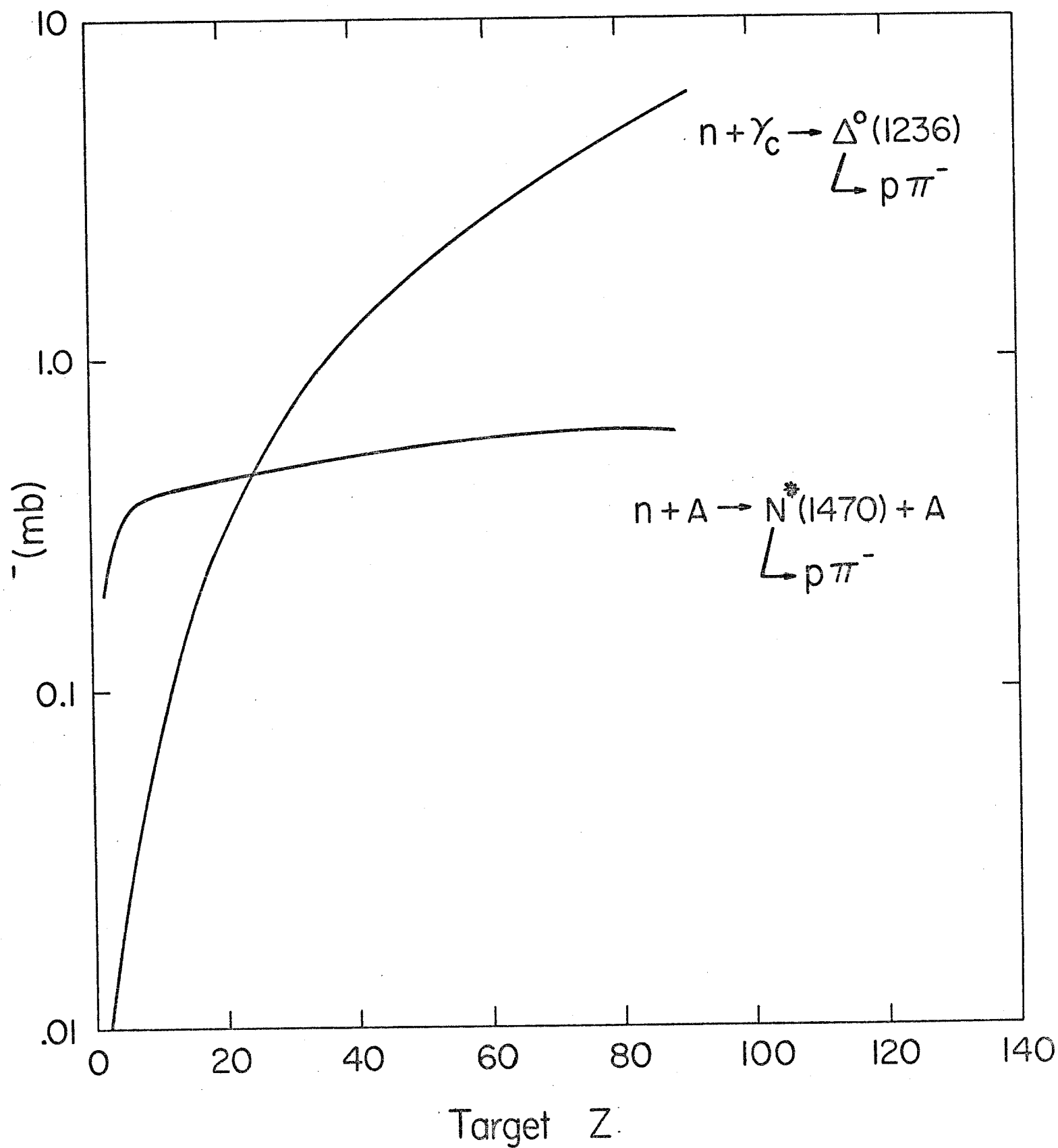


Fig. 1 Dissociation Cross Sections at 100 GeV

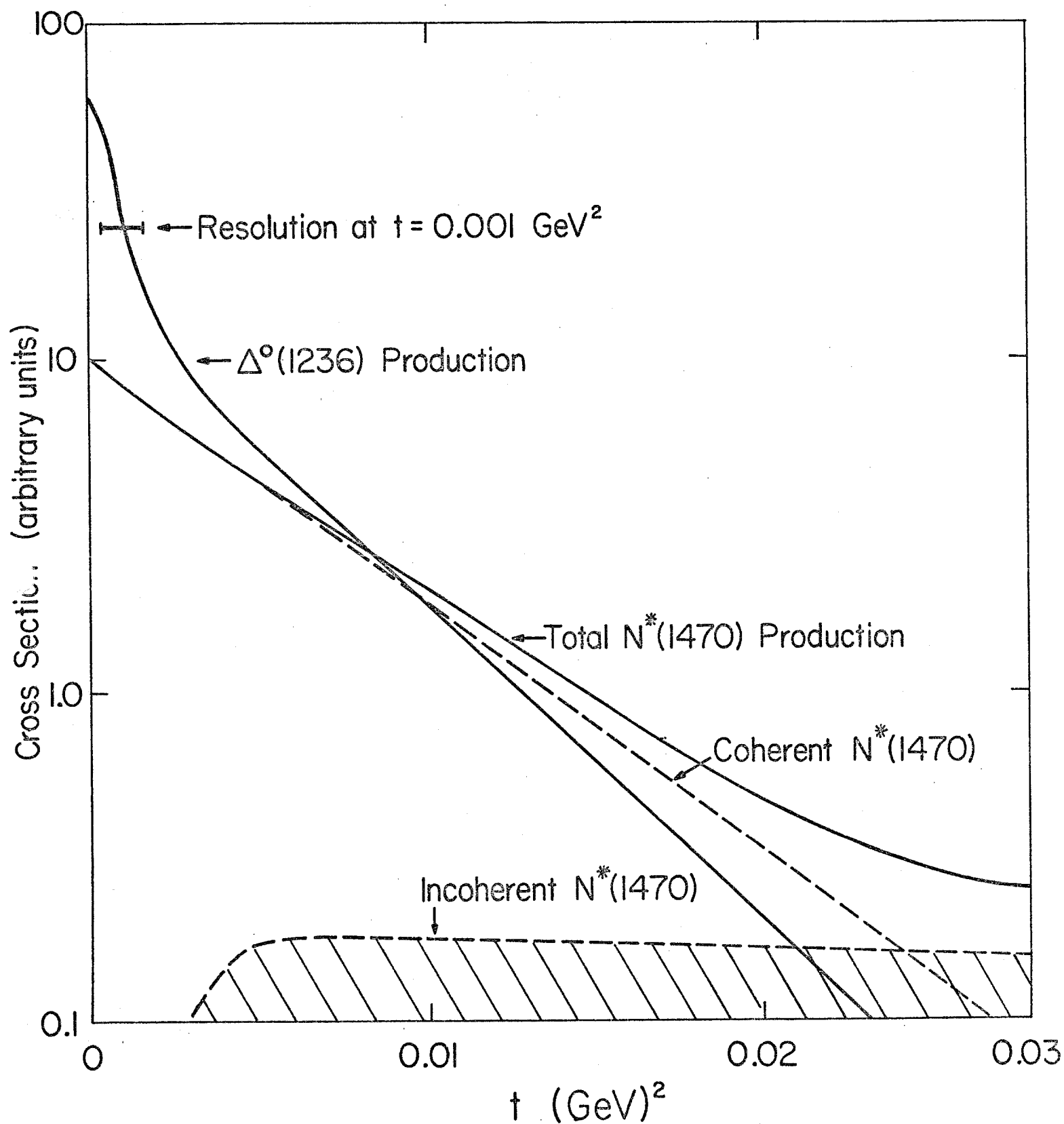


Fig. 2 Dissociation from Cu at 100 GeV

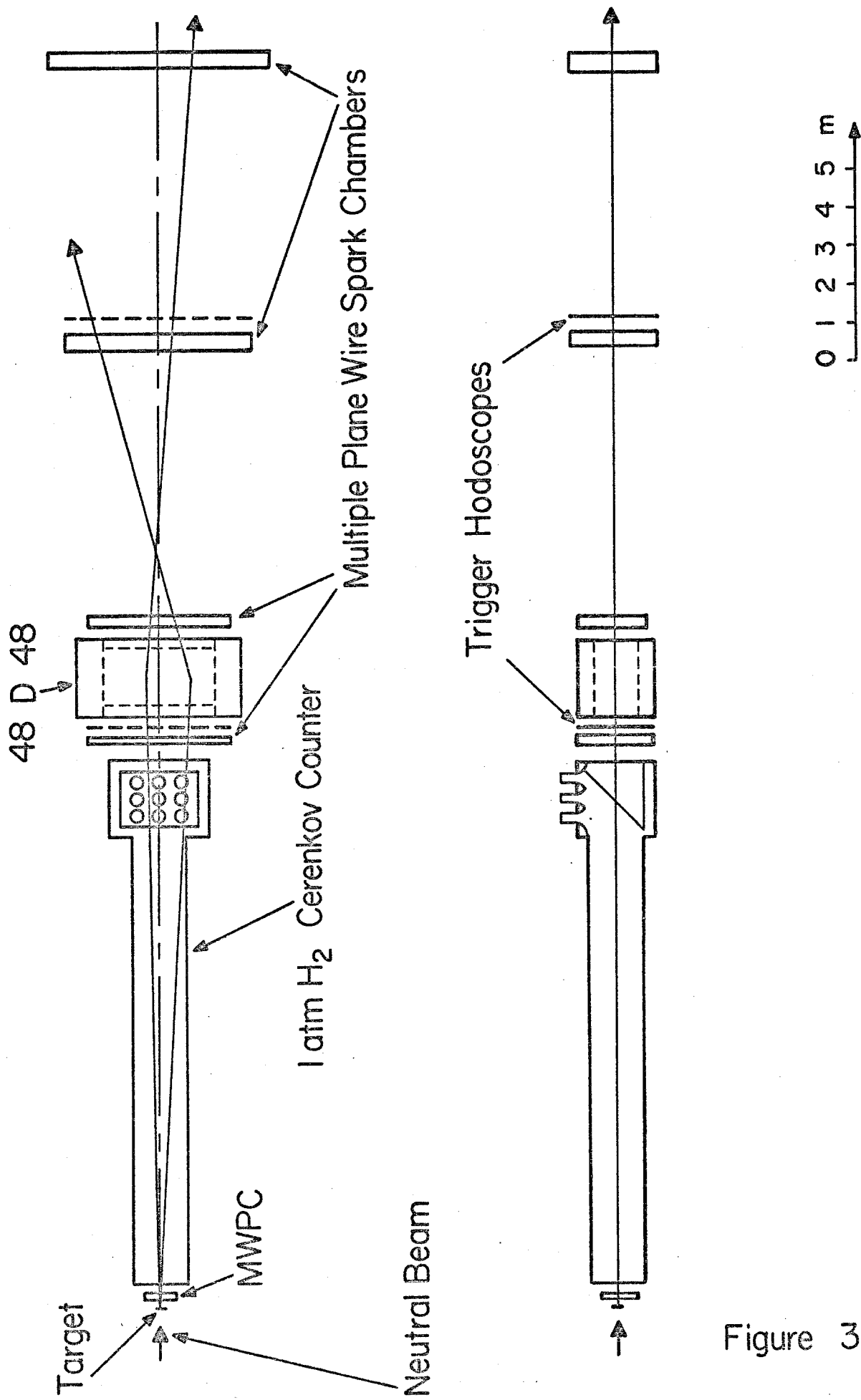


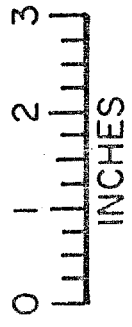


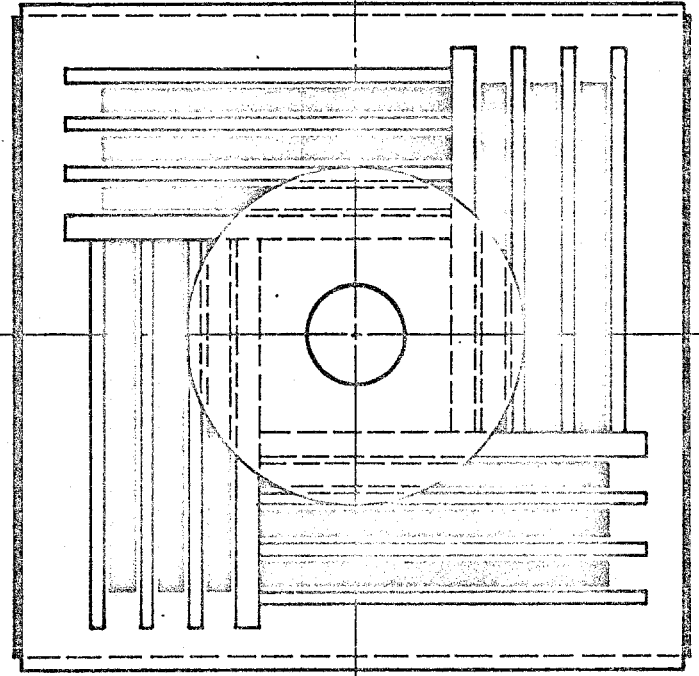
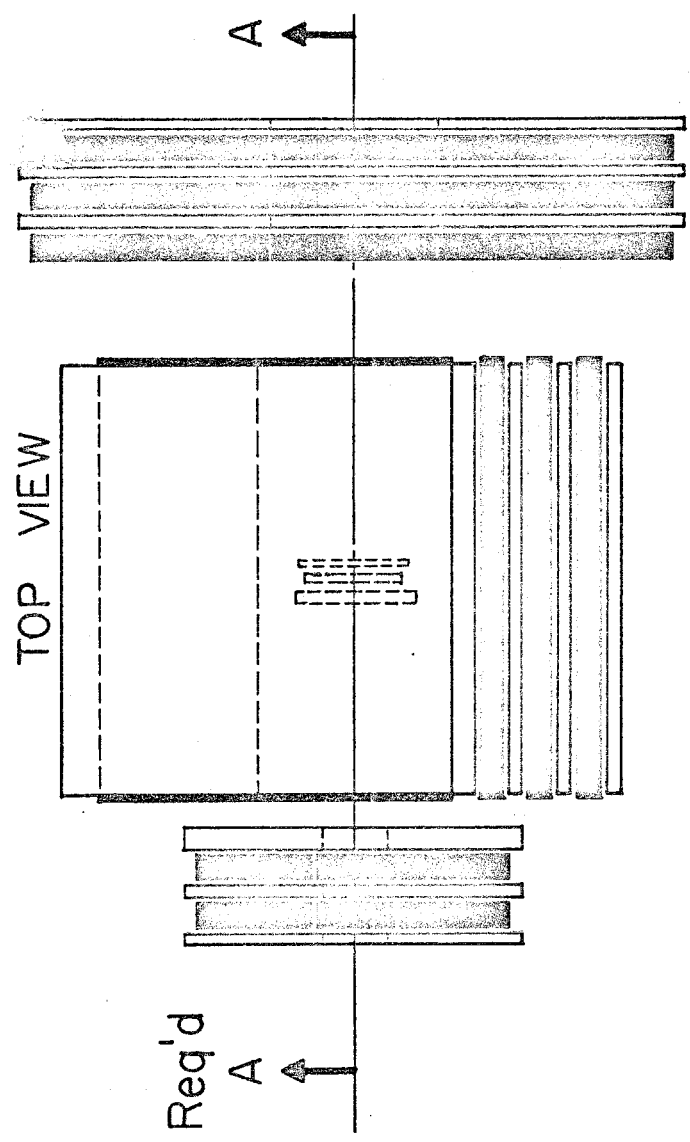
Figure 3

Veto Counters (Light Pipes Deleted) 7 P.M.'s Req'd

-  Pb
-  Scintillator



FRONT VIEW
LOOKING DOWNSTREAM



SECTION A-A

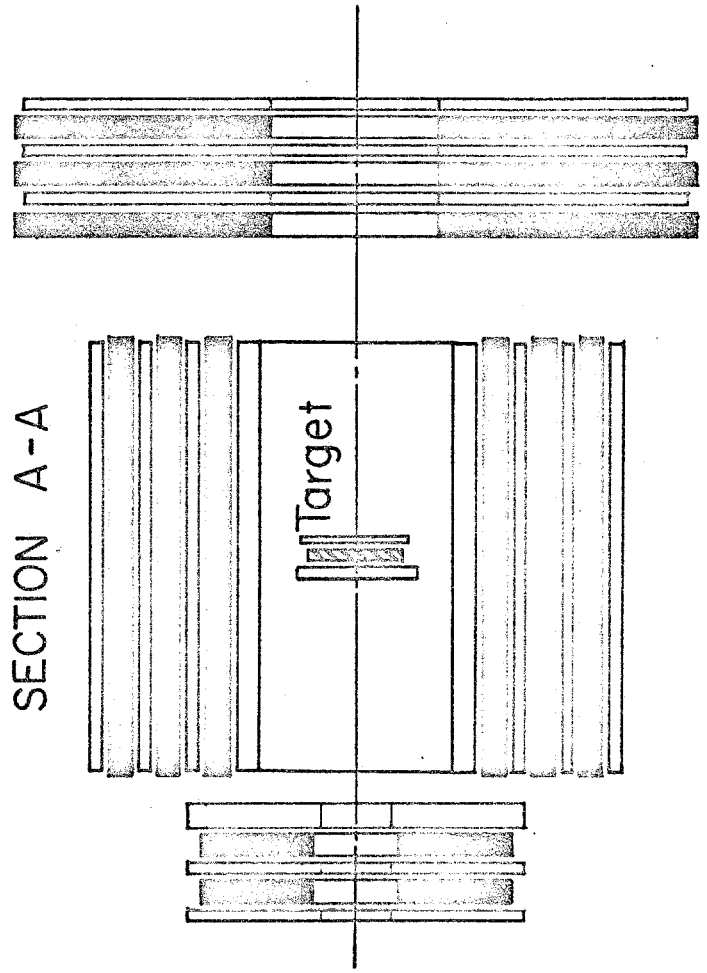


Figure 4

PROPOSAL TO STUDY THE COHERENT DISSOCIATION
OF NEUTRONS

T. Ferbel, B. Gobbi, J. Rosen, S. Shapiro, P. Slattery
and B. Werner, University of Rochester, E. J. Bleser,
National Accelerator Laboratory, S. L. Meyer and D. H.
Miller, Northwestern University

Correspondent: J. Rosen
Department of Physics
University of Rochester

ABSTRACT

At NAL energies, neutrons can be coherently excited by nuclei with appreciable cross section. By coherent we mean that the target nucleus recoils as a single entity without nuclear excitation. This neutron excitation can occur either by γ absorption in the nuclear Coulomb field (Coulomb dissociation) or by Pomeron exchange in the nucleus (diffractive dissociation). Both channels can result in the formation of $\pi^- p$ V's. We propose to study such V's using a spectrometer consisting of wire spark chambers, counters and analyzing magnet.

The two coherent processes can be identified and distinguished by their characteristic variation with neutron energy, momentum transfer, angular correlation, effective mass and A dependence. The former process (Coulomb) is dominated by $\Delta^0(1236)$ production while the latter is dominated by $N^*(1470)$ production. Coulomb dissociation is expected to be an order of magnitude more copious in high Z materials.

The objectives of the experiment are:

- 1) High statistics, comprehensive study of Coulomb and diffractive dissociation. Variations in momentum transfer, angular correlations and invariant mass (up to ~ 3 GeV) will be investigated as a function of target material and neutron energy (50-200 GeV).
- 2) Observe Coulomb and diffractive dissociation of the anti-neutron.

- 3) Survey the neutron and anti-neutron flux in the neutral beam.
- 4) Using transmission targets, measure neutron total cross sections as a function of energy.

I. Physics Justification

1) Coulomb Dissociation

The possibility that an elementary particle can be excited into a different state as a result of its interaction with the Coulomb field of a target nucleus was explored initially by Primakoff.⁽¹⁾ Subsequent calculations⁽²⁾ have elaborated on the rich physics consequences of this idea. In particular, Nagashima and Rosen⁽²⁾ have stressed that the Coulomb production of the $\Delta(1236)$, a process which can be calculated to great accuracy, can (1.) be used to test our understanding of the Primakoff process and thereby lend credence to the assumptions underlying our present knowledge of the π^0 and η^0 lifetimes, and (2.) be used to provide an efficient neutron detection scheme with excellent energy and directional properties.

The Coulomb production of $\Delta^0(1236)$ can be calculated in a rather straightforward manner.⁽²⁾ The differential cross section for the reaction:

$$n + \gamma_C \rightarrow \Delta^0(1236) \rightarrow \pi^- p \quad (1)$$

where γ_C refers to the photon from the nuclear Coulomb field of a high Z target material, is given by⁽³⁾:

$$\frac{d\sigma}{dt} = \frac{16\pi}{3} Z^2 \alpha \left(\frac{M}{M^2 - m^2} \right)^3 \Gamma_\gamma |F(t)|^2 \frac{(t - t_{\min})}{t^2} \quad (2)$$

where M and m are masses of the $\Delta(1236)$ and the neutron respectively, Γ_γ is the known radiative width of the Δ , F(t) is the nuclear form factor, α the fine-structure constant, and

Z is the nuclear charge. The integrated cross section for reaction (1) is rather substantial at present accelerator energies and, most importantly, grows significantly with increasing energy (essentially due to kinematic effects of t_{\min}). At 200 GeV/c, for example, approximately 0.5% ($\sim 7\text{mb}$) of the total interaction cross section for neutrons on Pb can be attributed to reaction (1). From expression (2) it is apparent that the natural width of the t -distribution in reaction (1) is typically of the order of t_{\min} . For 200 GeV/c neutron momentum, $\sqrt{t_{\min}} \sim \frac{M^2 - m^2}{2p} \sim 2 \text{ MeV/c}$. Thus the Coulomb peak is very sharp and its measured width will be determined by our apparatus which is capable of measuring transverse momenta with a sensitivity of $\sim 10 \text{ MeV/c}$.

2) Diffraction Dissociation

The nuclear diffraction dissociation phenomenon has been discussed extensively over the past few years⁽⁴⁾; and although several good experiments have been performed to study this process⁽⁵⁾, many quantitative questions regarding, for example, the amount of resonant contribution present in the dissociated system, the detailed nature of the energy dependence, and the phase of the diffraction dissociation amplitude, are still unanswered. The precise investigation of inelastic diffraction production processes, processes which are responsible for a large fraction of the observed total cross section in hadronic collisions, is clearly an important prerequisite to the understanding of strong interactions in general.

The differential cross section for neutron dissociation can be written as follows:

$$\frac{d\sigma}{dt} = \frac{d\sigma}{dt}_N A_{\text{eff}}^2 |F(t)|^2 \quad (3)$$

where $\frac{d\sigma}{dt}_N$ is the differential cross section for diffraction production (via $I = 0$ exchange without spin-flip) off a free nucleon, and A_{eff} can be regarded as the effective number of nucleons which take part in the coherent process ($A_{\text{eff}} \ll A$ for large nuclei because of the severe damping which hadrons experience in transversing nuclear matter. We estimate that for $N^*(1470)$ coherent production, for example, A_{eff} for C is ~ 5 , while for Pb it is ~ 15 .) The form factor of the nucleus can be parameterized in terms of the r.m.s. radius R :

$$|F(t)|^2 = e^{-\frac{R^2}{3}t} \quad (4)$$

with $R \sim 1.1 A^{1/3}$ fermi. Thus, the typical momentum transfer involved in the coherent diffractive dissociation of the neutron is $\sim (10 + 10A^{2/3})^{-1/2}$ GeV/c. For a Pb nucleus this corresponds to a transverse momentum of ~ 50 MeV/c, a momentum whose measurement is well within the resolution capability of our apparatus. For lighter nuclei, the typical transverse momenta in the diffraction dissociation process will be somewhat larger (for C it is ~ 140 MeV/c).

At NAL energies, the Coulomb production of $\Delta^0(1236)$ in high-Z materials dominates neutron diffraction dissociation (e.g., into the $N^*(1470)$ object), while the opposite is the

case for low-Z elements (see Fig. 1). Both processes are copious and both are characterized by an exceedingly steep t-dependence. In the case of the Coulomb process the inherent width of the forward momentum-transfer peak is determined essentially by the value of t_{\min} (not sensitive to the nuclear shape - $|F(t)|^2 \sim |F(0)|^2 \sim 1.0$), while the momentum transfer dependence in neutron diffraction dissociation has the width characteristic of the nuclear target radius. Figure 2 displays the relative shapes expected for the t-spectra for neutron dissociation (Coulomb and diffractive) off a medium-size nucleus, such as Cu. The width of the peak for the forward production of $\Delta^0(1236)$ has been broadened to account for experimental resolution.

It appears that the dissociation of a neutron into a $p\pi^-$ system, at the high energies available at NAL, will be a particularly tractable way to probe the nature of both the Coulomb dissociation and the nuclear diffraction dissociation phenomenon. A neutron which converts into a $p\pi^-$ "V" within a complex nucleus can readily be identified through the use of rather standard V-spectrometer detection systems (details described later). With an expected transverse momentum resolution of $\lesssim 10$ MeV/c, the kinematic separation of the $p\pi^-$ dissociation events from the background should prove to be a relatively easy task.

3) Survey of Neutron and Anti-Neutron Flux in the Neutral Beam.

An examination of Fig. 1 clearly reveals the previously noted fact that the $\Delta^0(1236)$ Coulomb production cross section in Pb is quite substantial. This suggests the possibility of using the $\Delta^0(1236)$ production mechanism in Pb as a reasonably efficient tool for neutron detection. The neutron and anti-neutron flux in the small angle neutral beam at NAL can be surveyed using a $\sim \frac{1}{4}$ radiation length Pb target (this is only $\sim \frac{1}{100}$ of an interaction mean free path). With a flux of $\sim 10^7$ neutrons/pulse we expect on the average a useful neutron conversion yield of ~ 100 counts/pulse. This rate is more than adequate for the neutron flux measurements, and should be sufficient to provide good data on the anti-neutron flux - particularly at lower energies (50 GeV) where the yield might be several percent of the neutron flux. The excited anti-neutron dissociates to an anti-proton and a π^+ and can be easily distinguished kinematically from the neutron dissociation.

4) Neutron Total Cross Section

By placing transmission targets in the beam far upstream of our V-spectrometer we plan to obtain better than 1% measurements of neutron total cross sections on hydrogen and on complex nuclei in 5 GeV/c momentum bands for the neutrons in the energy range between 50 GeV/c and 200 GeV/c. The anti-neutron measurements and a K_L^0 survey will be used to correct these precision cross sections.

The K_L^0 component of the neutral beam will be assayed through the measurement of the leptonic decays $K_L^0 \rightarrow \pi^\pm \mu^\pm \nu$. This can be achieved during one day of running time (the modification to the apparatus involves only minor changes).

The program involving the neutron studies described in the preceding pages is to be carried out in ~600 hours of data taking.

II. Experimental Equipment

The principal items which are required for the execution of this experiment are indicated schematically in Fig. 3. We will briefly describe these, and several other items of importance, in the order outlined below:

1. Neutral beam
2. Target and Target Counter System
3. Vertex Chamber
4. Gas Cerenkov Counter
5. Wide Aperture Magnet
6. Trigger Hodoscopes
7. Wire Spark Chambers
8. Dedicated Computer

1. Neutral Beam

A well-collimated, small-angle neutral beam is required. A flux of 10^7 neutrons in the momentum range of 50 GeV/c to 200 GeV/c, having a beam cross section of about $1-2 \text{ (inch)}^2$ at

1500' from the production target is suitable.

2.. Target, Target Counter System

For the study of the coherent nuclear and Coulomb dissociation reactions, we propose to use $1/4$ radiation length targets. Our minimum program will involve detailed investigations using Pb, Cu, Al, and C. These will be sandwiched between a $1/16$ " thick veto and a $1/32$ " thick trigger counter.

The target will be surrounded on all sides, except for entrance and exit holes on the beam axis, with a veto complex which will serve to suppress uninteresting nuclear reactions (large particle multiplicity or nuclear fragmentation). A schematic layout of the veto complex, which will shortly be used in a similar experiment at the AGS,⁽⁶⁾ is shown in Fig. 4. This arrangement has been constructed and was tested successfully at the AGS this past year. (In fact, it was on loan to Dr. Finocchiaro (SUNY) who used it in a diffractive scattering experiment carried out in a high flux π^- beam.)

For hydrogen and deuterium total cross section measurements we require a transmission target of (10-20)g thickness, located in the neutron tunnel. A cryogenic target - (4-8)' x 3" diameter would be adequate. A much simpler alternative is the use of a high pressure gas target. At normal storage cylinder pressure (2000lbs.) the target would have to be $\sim(20-40)$ ' long. It would be formed in several sections.

3. Vertex Chambers.

Following the target complex we will place a set of high-resolution ($<0.5\text{mm}$), horizontal and vertical, multiwire

proportional chambers. These will establish the initial transverse vertex coordinates of the V. They will present less than 50 mg of interaction material to the high-flux neutron beam. Approximately 200 wires will be involved. Testing of efficiency, stability, and reliability of the system is now underway in the laboratory and in a test beam at the AGS. The results have thus far been completely satisfactory.

4. Gas Cerenkov Counter

The bulk of the upstream region will be filled with a 15 meter 1 atmosphere threshold Cerenkov counter. The basic gas fill will be hydrogen. A $\beta = 1$ particle will provide 200 photons under these conditions and the Cerenkov angle will be 1° . The threshold energies will be 57, 30, 8.4 GeV for protons, kaons, and pions respectively. The total thickness of the hydrogen gas will be 0.15 g.

The counter will have thin mylar windows and a 45° stretched aluminized mylar mirror to reflect the light vertically where a hodoscope of photomultipliers and light gathering reflectors will be positioned.

It is proposed that this counter be constructed at NAL under the supervision of Drs. Bleser and Rosen. The cost should be under \$10K.

5. Wide Aperture Magnet

A 48D48 magnet will be suitable for the purposes of the present experimental design. With a gap of 18 inches, and an integrated field of 20 kG.m, this magnet will provide an

adequate transverse momentum kick of 0.6 GeV/c. Such a magnet costs approximately \$100K.

This magnet defines the limiting acceptance aperture, $\pm 9^\circ$ (V), $\pm 24^\circ$ (H). The corresponding acceptance for the magnet positioned at 17m from the target is ± 13 mrad (V) and ± 35 mrad (H).

6. Trigger Hodoscope

We will require 2 and only 2 charged particles passing through the system. This can be achieved through a rather straightforward triggering arrangement. The hodoscope information should also prove to be valuable in the pattern recognition of the wire spark chamber data.

7. Wire Spark Chambers

We have already constructed one of the multiple plane systems and are presently testing it (the chambers have useful areas of 46" x 92").

We wish to point out that we have extensive experience with this technique. We recently completed an experiment which recorded five million triggers and employed 12 wire planes. The chambers were completely fabricated in Rochester. (We are equipped to wind chambers of arbitrary size.) Data were produced with the aid of the Rochester-owned Honeywell DDP-516 computer and ancillary magnetostrictive equipment.

8. Dedicated Computer

The Rochester Group has recently purchased a PDP-15 system (now delivered) which will be available for this experiment. We request a link to a large time-sharing central

computer for selective on-line analysis. If this is not available, then off-line fast turn-around on a large NAL computer (\sim PDP-10) will be required.

III. Technical Details

1. Yields and Detection Efficiency

The envisioned neutron dissociation studies on C, Al, Cu and Pb, as well as the flux and total cross section measurements, will have substantial event rates. For the flux measurements, for example, we plan to use a 1.5 gm/cm^2 Pb target. As noted previously, the useful cross section for the Coulomb process (reaction 1), in the 50 GeV/c to 200 GeV/c momentum range, is about 5 mb/Pb nucleus. This gives an event rate of $\sim 300 \text{ p}\pi^-/\text{pulse}$. The detection efficiency of the $\text{p}\pi^- \text{ V}$ is largely determined by the solid angle acceptance of the magnet. These efficiencies have been evaluated with standard Monte Carlo techniques and are shown in Fig. 5. On the whole, the acceptance is large, and, in particular, for the Coulomb-produced $\Delta^0(1236)$ the efficiency will be $\sim 50\%$ for the entire neutron momentum range. The estimated yield of ~ 100 useful V's per 10^7 neutrons (one pulse) is sufficiently large for the precision measurement of neutron total cross sections and for a less accurate determination of anti-neutron cross sections.

2. Background

Although the useful yield of high energy $\pi^- \text{ p}$ pairs from the Coulomb process is $\sim 5 \text{ mb}$, it must be noted that the Pb interaction cross section is approximately geometric, i.e.,

~ 1500 mb. Now the great bulk of this cross section results in very large multiplicity and nuclear fragmentation events. In our background estimates we conservatively estimate that only the outer rim of ~ 500 mb projected area can be regarded as hydrogen-like, i.e., free of secondary interactions, reabsorption and remultiplication. (At A.G.S. energies it is observed that pp collisions result in single energetic $N\pi$ pairs for less than 1% of the interactions). Thus we expect trigger background from the nuclear rim with an effective cross section of a few mb or less. The incoherent background will cause no trouble in the analysis of the dissociation data since the t-spectrum from these events will be considerably flatter than from coherent interactions (see Fig. 2). Direct experimental data bearing on this point will be available shortly from the A.G.S. experiment. (6)

3. Resolution

The final kinematical analysis will involve the wire chamber measurement of π^- and p momenta. The coherent events will be signaturred by a sharp peak on a plot of events versus transverse momentum transfer. The sharp peak will be largely contained inside $q(\text{transverse}) \sim 100$ MeV/c. Incoherent background will have an average $q(\text{transverse}) \sim 300$ MeV/c. The expected angular resolution is $\sim 1 \text{ mm}/20\text{m} = 5.0 \times 10^{-5}$ rad, while the momentum resolution will be $\sim 1\%$. A 100 BeV/c proton, for example, will bend by $(0.6 \text{ BeV/c}/100 \text{ BeV/c}) = 6 \text{ mrad}$. This gives $\delta p/p = \delta\theta/\theta \sim 1\%$.

The uncertainty in p (transverse) resulting from angle uncertainty will be $p \delta\theta \sim 5 \text{ MeV/c}$. The actual limit on transverse momentum resolution comes from multiple Coulomb scattering, principally in the $1/4$ radiation length target. There are two particles produced on the average $1/2$ of the way into the target. Therefore, the uncertainty in the transverse momentum produced by the target is $\sim 10 \text{ MeV/c}$. Thus we see that the transverse resolution is adequate for resolving the sharp coherent spike.

The N^{*0} mass resolution is excellent. This can be inferred from the formula for the mass

$$\begin{aligned} m_{N^*}^2 - (m_p^2 + m_\pi^2) &= 2(E_p E_\pi - \vec{p}_p \cdot \vec{p}_\pi) \\ &= p_\pi p_p \left(\frac{m_\pi^2}{p_\pi^2} + \frac{m_p^2}{p_p^2} + \theta^2 \right) \end{aligned}$$

where $\theta = V$ opening angle. It is readily shown that

$\delta m_{N^*}/m_{N^*} \sim 1\%$, using the previously noted uncertainties on angle and momentum measurements.

It is interesting to note that this high mass resolution is achieved with a relatively small $\int B \, d\ell$. The opening angle of the V plays the crucial role. This is in sharp contrast with missing mass work for example, where the mass measurement depends on the differences in the momenta of incoming and outgoing particles.

Our analysis of the efficiency, resolution and separation of the aggregate coherent events should be regarded as proceeding along well established lines. Precisely the same considerations have been employed in successful experiments on

(a) coherent K_S^0 regeneration, and (b) diffractive ρ^0 production in photon beams. Both types of experiments study $\pi^+\pi^-$ V's produced in beams with wide band primary momentum distributions. Our yields per incident particle compare quite favorably with these experiments.

References

1. H. Primakoff, Phys. Rev. 81, 899 (1951).
2. M. Good and W. Walker, Phys. Rev. 120, 1855 (1960);
C. Chiuderi and G. Morpurgo, Nuovo Cimento 19, 497 (1961);
V. Glaser and R. A. Ferrell, Phys. Rev. 121, 886 (1961);
I. Pomeranchuk and I. Shmushkevich, Nucl. Phys. 23, 452
(1961); S. M. Berman and S. D. Drell, Phys. Rev. 133,
791 (1964); C. A. Englebrecht, Phys. Rev. 133, 988 (1964);
A. Halprin, C. M. Anderson, H. Primakoff, Phys. Rev. 152,
1295 (1966); Y. Nagashima and J. Rosen, University of
Rochester Report UR-875-295 (1969).
3. See the report of Nagashima and Rosen for details.
4. M. Good and W. Walker, Phys. Rev. 120, 1857 (1960); I. Pomeran-
chuk and I. Shmushkevich, op. cit.; M. Ross and Y.Y. Yam, Phys.
Rev. Letts. 19, 546 (1967); E. L. Berger, Phys. Rev. Letts.
21, 701 (1968); G. Chew and A. Pignotti, Phys. Rev. Letts.
20, 1078 (1968); also see report by H. H. Gingham, loc cit
for other references.
5. A. M. Cnops et.al., Phys. Rev. Letts. 25, 1132 (1970), and
references cited therein; C. Bemporad et.al., CERN preprint
(Kiev Conference-1970); R. Huson et.al., Nucl. Phys. B8,
391 (1968); Also see recent review paper by H. H. Bingham,
CERN Report D.Ph.II/PHYS/70-60.
6. An experiment on $\pi^- + \gamma_c \rightarrow \rho^-$ and $p + \gamma_c \rightarrow \Delta^+$ is scheduled to
begin this spring at the A.G.S. The Rochester group will
carry out this experiment using the Lindenbaum-Ozaki
spectrometer. Triggering tests, which have relevance to

References continued

the present proposal, were satisfactorily completed during the summer of 1970. Using an 8 BeV/c π^- beam and a simulated triggering arrangement, including the target veto counter complex, we looked for ρ^- -like triggers originating from 1/4 radiation targets of Pb, Cu, and Al. Our expectations concerning incoherent trigger background were confirmed. Detailed results will be provided upon request.

Figure Captions

- Fig. 1. Z dependence of the dissociation cross sections at 100 GeV/c for the reactions $n + \gamma_c \rightarrow \Delta^0(1236) \rightarrow p\pi^-$ and $n + A \rightarrow N^*(1470) + A \rightarrow p\pi^- + A$.
- Fig. 2. Expected relative shape for the t-spectra for neutron dissociation (Coulomb and diffractive) off Cu.
- Fig. 3. The proposed experimental layout.
- Fig. 4. Target arrangement.
- Fig. 5. Spectrometer acceptance. The percentage of N^* decays accepted by the V-spectrometer as a function of N^* mass for initial neutron momenta of 50, 100, 150 and 200 GeV/c.

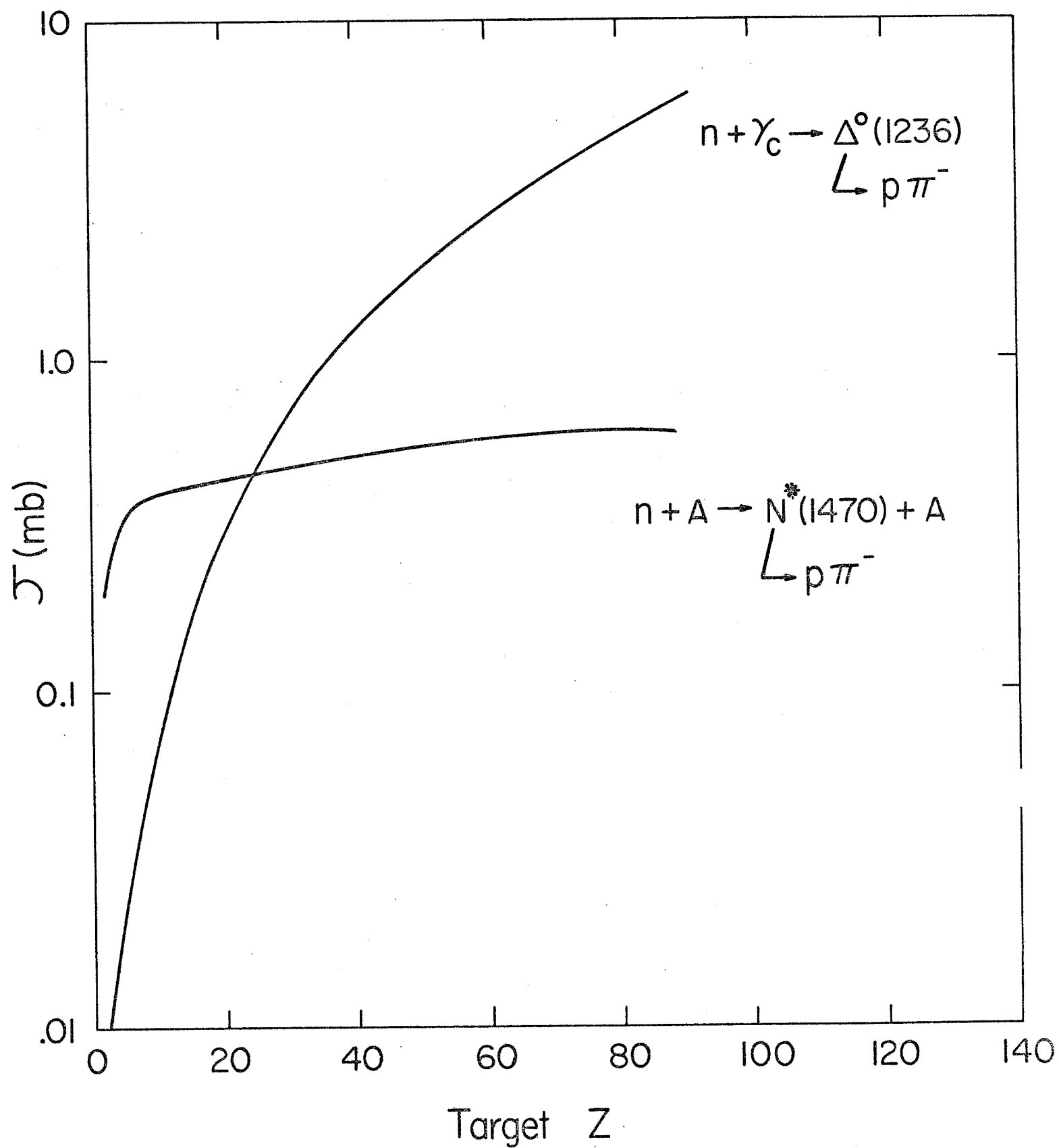


Fig. 1 Dissociation Cross Sections at 100 GeV

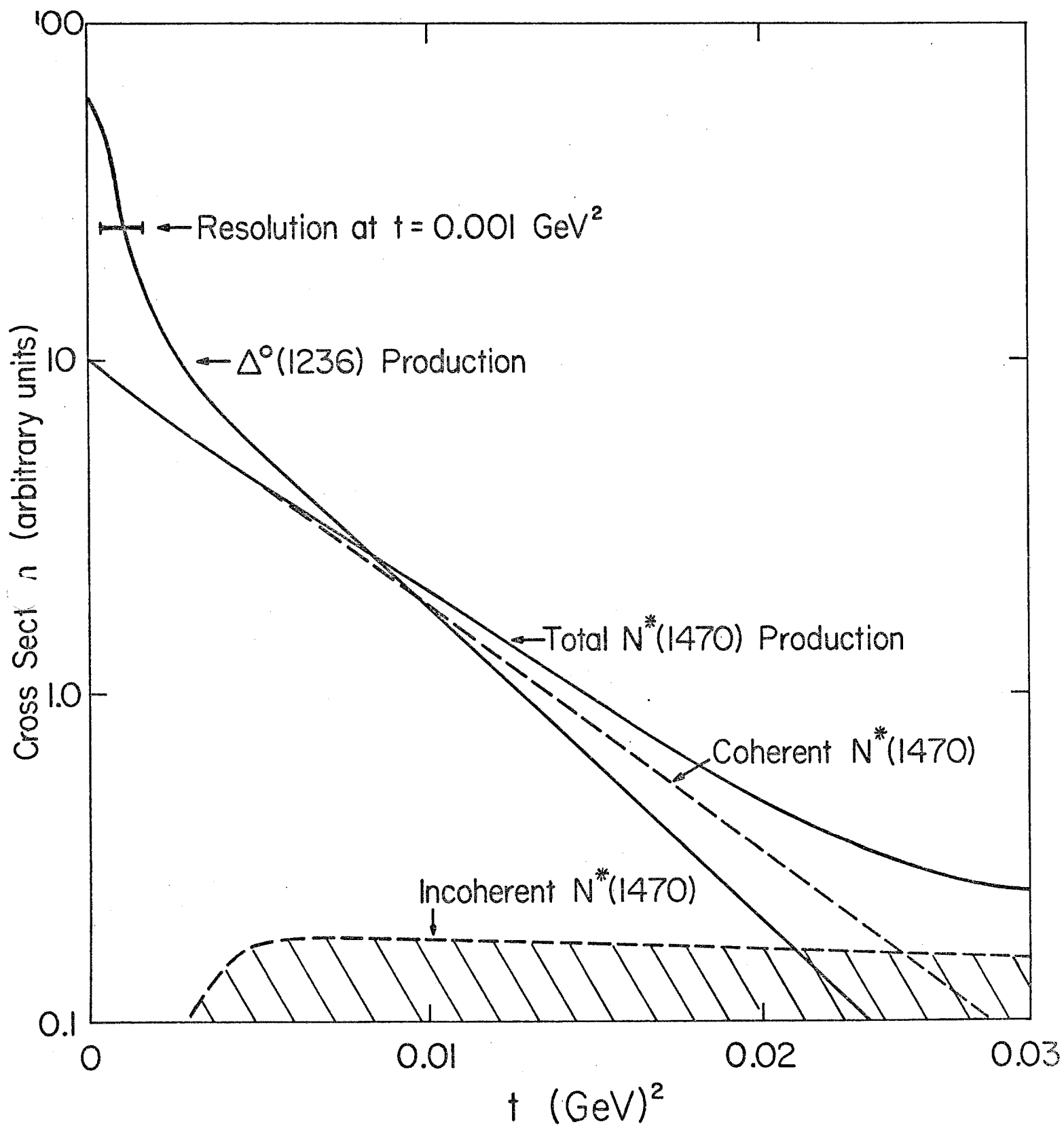


Fig. 2 Dissociation from Cu at 100 GeV

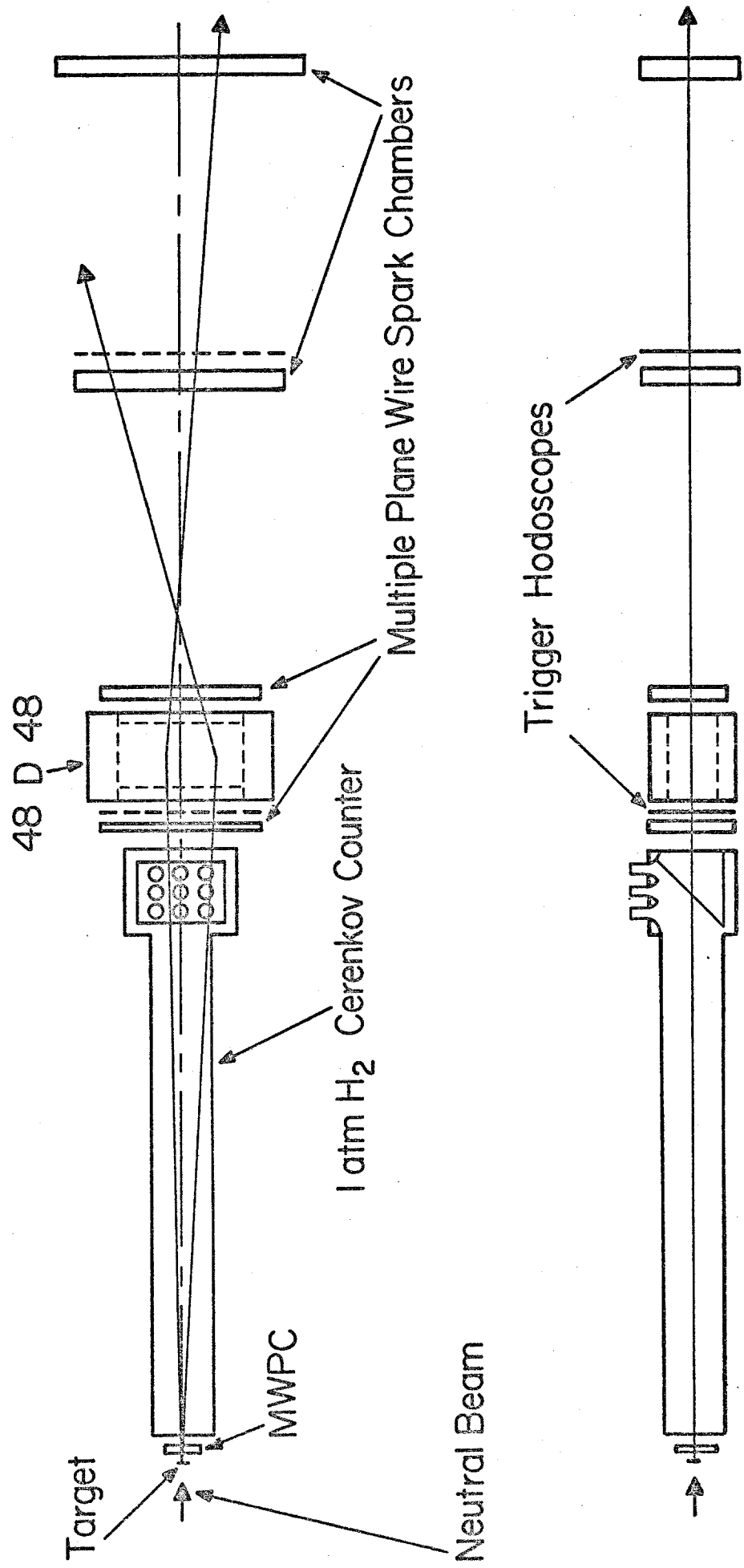




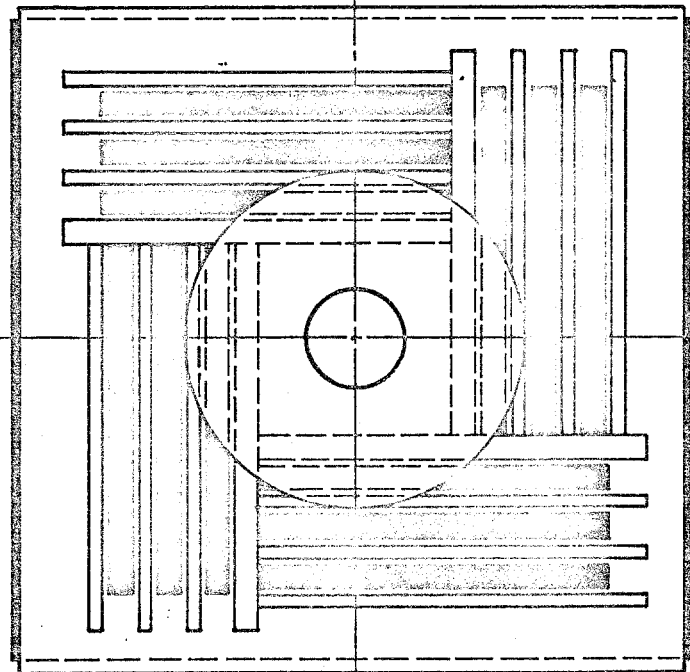
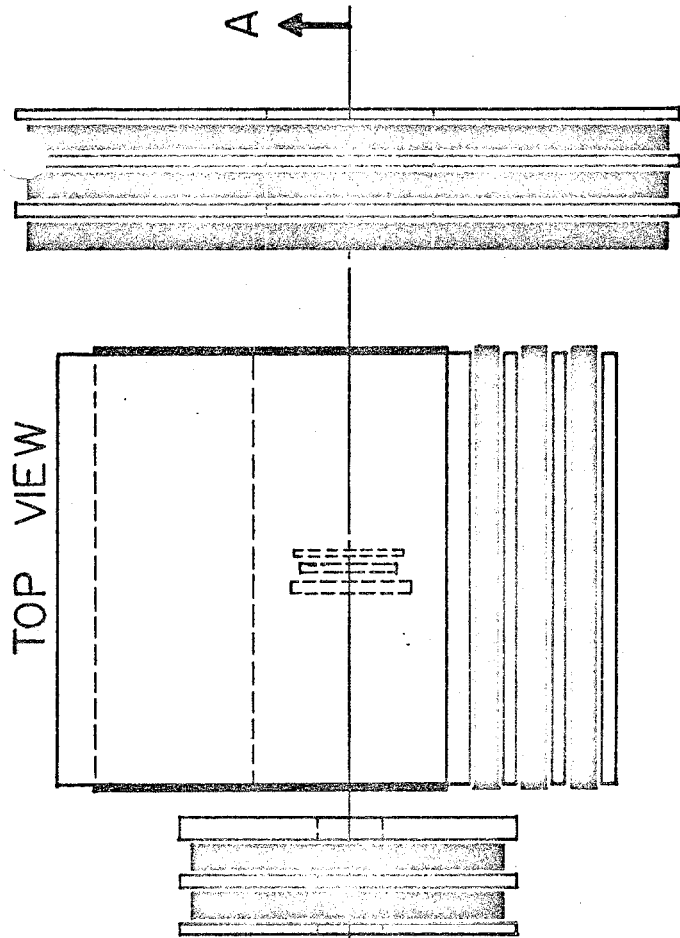
Figure 3

Veto Counters (Light Pipes Deleted) 7 P.M.'s Req'd

 Pb
 Scintillator

0 1 2 3
 INCHES

FRONT VIEW
LOOKING DOWNSTREAM



SECTION A-A

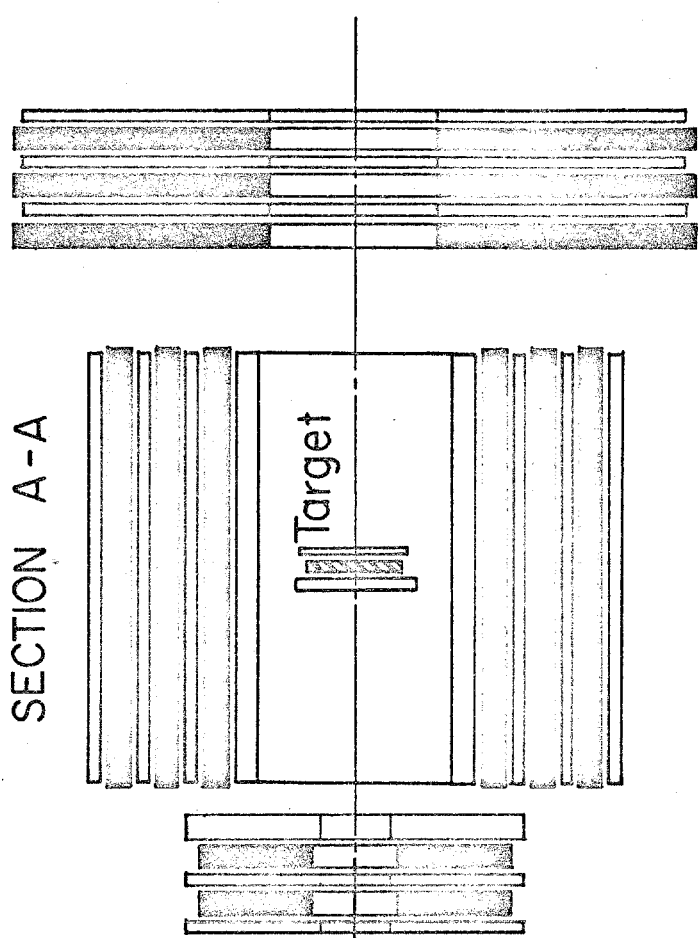


Figure 4

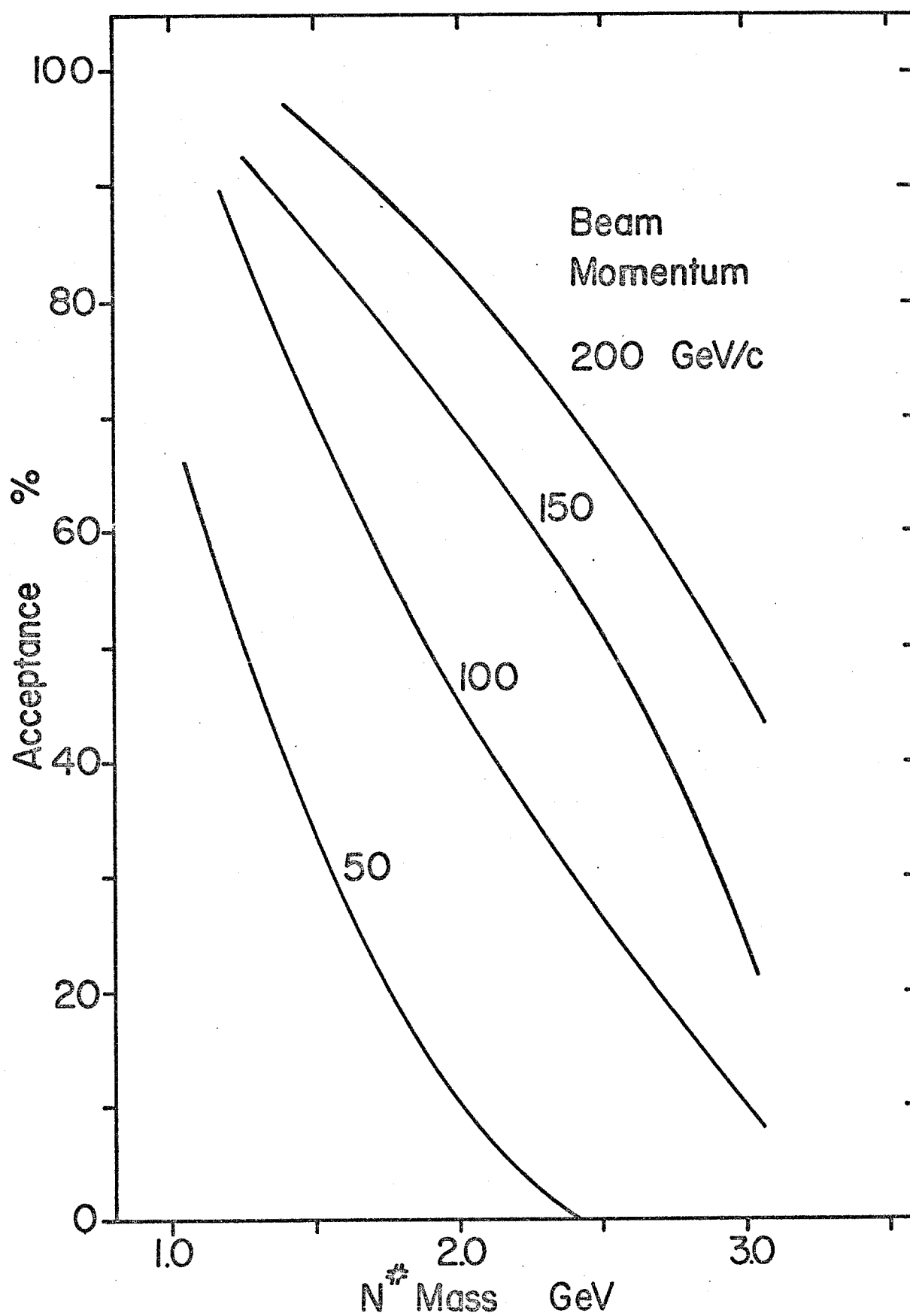


FIG. 5 Spectrometer Acceptance